~~CONFIDENTIAL~~

Department of the Navy
Bureau of Ordnance
Contract No, NOrd 9612

DRAG STUDIES IN WATER ENTRY

OF THE

MK 13-6 TORPEDO

Report No. E 12.1
July 1951

Hydrodynamics Laboratory
California Institute of Technology

~~CONFIDENTIAL~~

Department of the Navy
Bureau of Ordnance
Contract NOrd-9612

DRAG STUDIES IN WATER ENTRY OF THE MK 13-6 TORPEDO

by

Genevieve M. Wilcox
Research Engineer

Hydrodynamics Laboratory
California Institute of Technology
Pasadena, California

Report No. E 12.1
Copy No. 94

Joseph Levy
Project Supervisor

TABLE OF CONTENTS

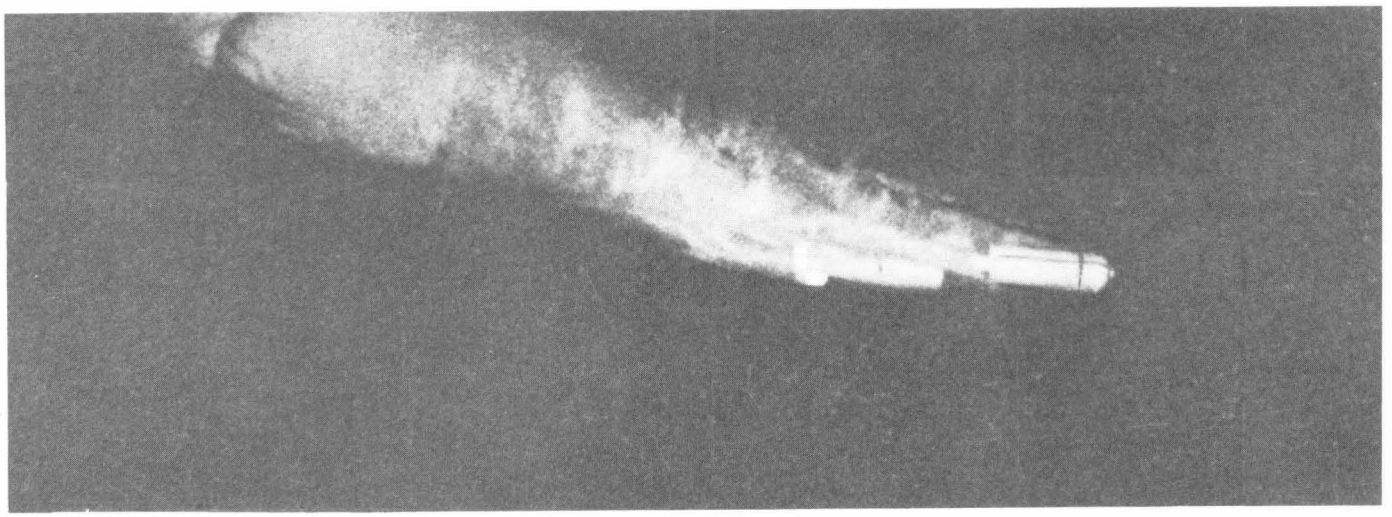

The model of the standard Mk 13-6 aircraft torpedo during the cavity phase of the underwater trajectory

ABSTRACT

An experimental investigation was made of the drag characteristics of a 2-in. diameter model of the standard (Head F) Mk 13-6 torpedo during the cavity phase of the underwater trajectory. The data used in this analysis were available from a previously completed trajectory study. These data were sufficient to determine the instantaneous velocity of the model along its trajectory. Hence, the deceleration and the instantaneous drag coefficient could be determined.

The model was dynamically and geometrically similar to the prototype; its entry velocity of 120 fps was scaled from the prototype velocity of 406 fps in accordance with the Froude law. Results from model runs made at nominal atmospheric pressures of 1, 1/2, 1/11, and 1/22 atmospheres with initial pitches between $\pm 6^{\circ}$ are presented. A fixed trajectory angle of 19° was used in all tests. Prototype data from the Naval Ordnance Test Station, Morris Dam, taken at a nominal trajectory angle of 19° with initial pitches between $\pm 1^{\circ}$ were available for comparison.

Results from three tests of the Mk 13-6 torpedo model with the finer Dunn nose (Head I) made at air pressures of 1, 1/11, and 1/22 atm. are also presented. These runs were made with a nominal trajectory angle of 20° and entry velocity of 120 fps with initial pitches between $\pm 0.5^{\circ}$. There were no prototype data from this shape suitable for drag analysis.

The results of the investigation are summarized in the conclusions at the end of the report.

INTRODUCTION

An investigation of the water entry of small-scale projectiles was undertaken at the Hydrodynamics Laboratory of the California Institute of Technology in an effort to develop a satisfactory modeling technique and to study the behavior of air-launched projectiles under a wide range of entry conditions. This study was jointly sponsored by the Bureau of Ordnance and the Office of Naval Research under Contract NOrd 9612.

General Discussion of Water Entry

When an air-launched torpedo strikes the water it creates a cavity which persists into the underwater trajectory. The analysis of the drag during the cavity stage is facilitated by observing the orientation of the model as it moves along the trajectory. During the cavity phase the torpedo may do one of three things (Fig. 1): (1) it may travel with only its nose in contact with the water, (2) it may travel with its nose in contact with the water and its afterbody oscillating between the top and bottom of the cavity, (3) or it may travel with both its nose and afterbody in contact with the cavity wall. If the first or second condition exists, the mean trajectory is the straight line extension of the air path. The third condition, which most often occurs, produces a trajectory convex toward the side of the cavity in contact with the tail. The drag will be lower when only the nose of the torpedo is in contact with the water. When other portions of the torpedo in addition to the nose contact the cavity wall, the cavity bulges at the point of contact causing the cross section of the cavity and, hence, the drag to increase. In general, the drag on the torpedo will be greater during the cavity phase than it is when the torpedo is completely in contact with the water.

Froude scaling has been used in the modeling of water entry because the forces of gravity and inertia are of major importance during the cavity phase of the trajectory. This modeling system is not valid beyond the cavity phase because the viscous forces become significant after the cavity has been dissipated. Theoretical considerations further indicate that valid modeling also requires equal cavitation numbers in the model and prototype systems. The cavitation number is defined as:

$$k = \frac{p_o - p_c}{1/2\,\rho v^2}$$

where:

p_o = absolute static pressure in the undisturbed liquid
p_c = absolute pressure within the cavity
v = velocity of the torpedo
ρ = density of water

In order to fulfill the requirement of equal cavitation numbers, the atmospheric pressures in the model and prototype systems must be in the same ratio as the linear dimensions of the model and prototype.*

Much of the early work in the modeling of water entry was done with models of the standard Mk 13-6 aircraft torpedo launched in open tanks. These tests indicated that simple Froude scaling was sufficient to reproduce the trajectory of that projectile. However, when the finer Dunn nose was substituted for the standard head of the torpedo, the model followed a steeply diving trajectory in contrast to the level path of the prototype. It was necessary to reduce the air pressure in the model system before the prototype trajectory could be satisfactorily reproduced.[1, 2, 3]** Several nominal air pressures were investigated with the fine nosed model. At 1/11 atm., where the cavitation number was equal in both model and prototype systems, the model trajectories fell within 5 calibers of the prototype trajectory for the first 70 calibers of horizontal travel. At air pressures of 3/4, 1/2, 1/4, and 1/22 atm., the model trajectories deviated more widely from those of the prototype. Therefore, these results support the theoretical evidence that equal cavitation numbers should be a criterion for valid modeling.

Purpose

Modeling of trajectory implies but does not prove that drag has been modeled as well. The purpose of the investigation was to determine whether drag was satisfactorily modeled by Froude scaling and to ascertain the effect of atmospheric pressure upon the drag characteristics of the model. Since the only prototype data available were from the standard Mk 13-6 torpedo, a shape relatively insensitive to atmospheric pressure at model size, the results

*Appendix III includes a discussion of the important factors in modeling.

**Numbers in superscript refer to bibliography at the end of this report.

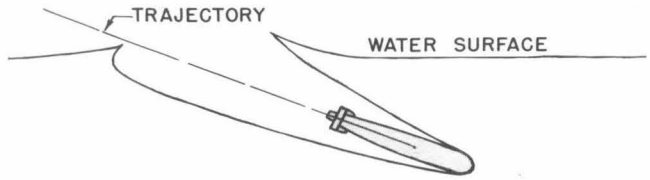

A. ONLY NOSE CONTACTING WATER

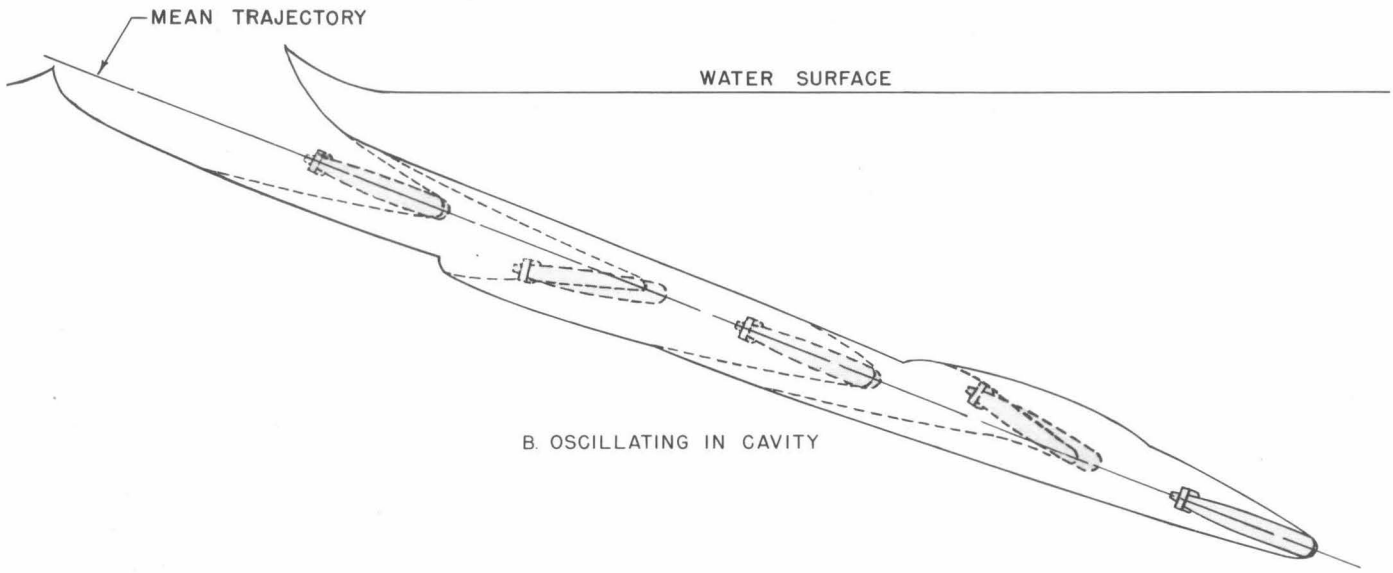

B. OSCILLATING IN CAVITY

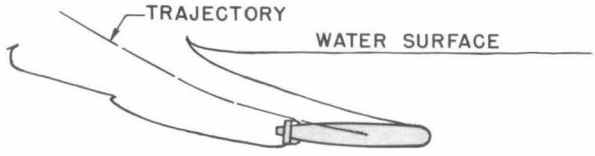

C. CONTACTING BOTTOM OF CAVITY

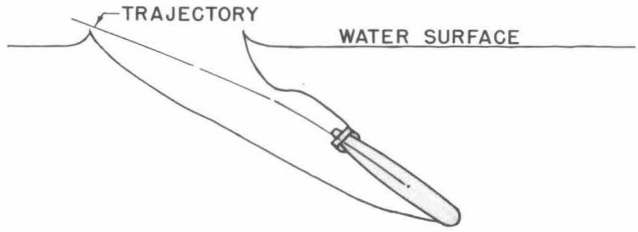

D. CONTACTING TOP OF CAVITY

Fig. 1 - Orientation of the torpedo in the cavity.

of this study could only establish the validity of Froude modeling and give some indication of the region in which the most satisfactory air pressure might lie.

The model data taken at nominal air pressures of 1, 1/2, 1/11, and 1/22 atm. were available from the previously completed trajectory study. The test results from two typical runs from each pressure condition were analyzed to determine the drag on the model. Both these and the prototype tests were made with initial pitches between $\pm 1^{o}$. Since it was hoped that this drag study could establish some trends in model behavior that would be of use in later work with more sensitive projectiles, the initial pitch range investigated at air pressures of 1 atm. and 1/11 atm. was extended from $\pm 1^{o}$ where comparison with the prototype was possible to $\pm 6^{o}$. Data from the pressure sensitive Dunn nose torpedo launched with essentially constant entry pitch and velocity, but with air pressures of 1, 1/11, and 1/22 atm., were also included even though prototype comparison was impossible.

Experimental Program

Models

The two models used in these tests were of the Mk 13-6 torpedo. One was of the standard Head F torpedo with the spherical-tip-and-cone nose, and the other was of the Head I torpedo, a finer shape also known as the Dunn nose (Fig. 2). Both models were 2-in. in diameter, geometrically and dynamically scaled from the 22.42-in. diameter "floater" torpedo used in the prototype work.[4] The details of model construction and tolerances for the physical constants are given in Appendix I.

Test Conditions

The models were launched at nominal air pressures of 1, 1/2, 1/11, and 1/22 atm. An air pressure of 1/11 atm. will produce equal cavitation numbers in both model and prototype systems. The entry velocities of the models varied between 116 and 122 fps; (120 fps corresponds to a Froude scaled prototype velocity of 406 fps). The tests were made with initial pitches ranging from 6.4^{o}S (S denotes steep or nose down with respect to the trajectory) to 5.3^{o}F (F denotes flat or nose up with respect to the trajectory), at nominal trajectory angles of 19^{o} for the standard torpedo and 20^{o} for the Head I. The launching conditions of the individual runs are tabulated in Table I.

Determination of Drag

Drag was determined from deceleration of the model along its trajectory. The methods

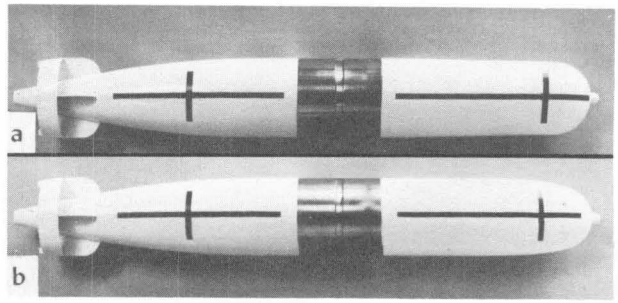

Fig. 2 - The Mk 13-6 torpedo model
(a) The model with the standard hemisphere-and-cone nose (Head F)
(b) The model with the finer Dunn nose (Head I)

TABLE I. LAUNCHING CONDITIONS
Mk 13-6 TORPEDO MODELS

Run No.	Tank Air Pres. Std. Atms.	Entry Velocity fps	Entry Pitch o	Angles Traj. o
Standard Mk 13-6 Torpedo (Head F)				
9-1	0.984	120.6	0.1F	18.9
9-2	0.515	122.1	0.3S	18.3
9-3	0.046	119.9	0.2F	18.6
9-4	0.035	120.1	0.6S	19.2
9-5	0.514	119.2	1.0S	18.5
9-6	0.979	117.9	1.1S	18.6
9-28	0.977	120.9	2.6S	18.1*
9-30	0.978	119.2	6.0S	18.4
9-32	0.089	115.9	6.4S	19.0*
9-39	0.500	117.2	2.5S	19.5
9-40	0.045	119.9	1.7S	19.1
9-41	0.089	119.5	2.0S	18.8
9-42	0.089	120.2	0.8S	18.8
9-43	0.089	117.8	0.1S	18.8
9-51	0.967	121.3	3.0F	18.3
9-52	0.089	121.3	3.6F	18.8
9-53	0.975	121.9	5.2F	18.6
9-54	0.089	121.2	5.3F	18.7
Mk 13-6 Torpedo with Dunn Nose (Head I)				
11-14	0.089	121.6	0.2S	20.1
11-16	0.045	121.5	0.5F	20.5
11-23	0.978	120.4	0.3S	20.3*

*Possible error $\pm 0.5^{o}$; all other trajectory angles correct to $\pm 0.2^{o}$.

of calculation and the assumptions used in reducing the basic trajectory data are given in Appendix II. The data used in this analysis are from photographic records of the launchings made in the Controlled Atmosphere Launching Tank.*

EXPERIMENTAL RESULTS

Model and Prototype Drag Comparisons

The prototype data presented in this report were taken at the Naval Ordnance Test Station at Morris Dam. The tests were made with the "floater" version of the 22.42-in. Mk 13-6 aircraft torpedo.[4] This projectile is a full-scale buoyant model of the standard Mk 13-6 torpedo without engine or steering mechanism.

Instantaneous drag coefficients could not be determined from the prototype data. Therefore, comparison was made between the curves which resulted when the logarithm of the instantaneous velocity was plotted against the distance from entry. The slope of these curves at any point is proportional to the instantaneous drag coefficient (see Appendix II). Figures 3 and 4 show the logarithm of the ratio of the instantaneous velocity to the entry velocity plotted against the distance from entry in calibers. Model data taken at air pressures of 1, 1/2, 1/11, and 1/22 atm. are compared with the prototype results.[5,6] These tests were made within an initial pitch range of $\pm 1^{o}$. The agreement between model and prototype is good to a distance of about 50 calibers from entry. Beyond 50 calibers the model was retarded more rapidly than the prototype. The model data taken at 1/2 atm. and 1/11 atm. are in closest agreement with the prototype results, indicating the best pressure for modeling to be in this region. The results from the 1/22 atm. tests deviated most widely from those of the prototype.

The curves which resulted when the distance traveled from entry was plotted against time were also compared, as a greater distance traveled in a given time represents a lesser drag. Figures 5 and 6 show the distance from entry in calibers plotted against prototype time. These curves substantiate the trends in model behavior which were evident in the curves of Figs. 3 and 4.

Drag of the Standard Mk 13-6 Torpedo Model

Variation of Drag Along the Trajectory

The model test data were sufficient to determine the instantaneous drag coefficients. When only the nose of the projectile was contacting the cavity wall, 85% of the instantaneous drag coefficients were between 0.18 and 0.30. The maximum and minimum values were 0.36 and 0.15, respectively. This coefficient should be comparable to that of the hemisphere at zero cavitation number $(C_d)_0$ because the flow separates on the hemispherical portion of the nose and the cavitation number is essentially zero. (The depth of submergence is small and the velocity high during this portion of the trajectory.) The value of $(C_d)_0$ is approximately 0.22* and, hence, in reasonable agreement with the measured values.

The first contact of the torpedo tail with the cavity wall (tail slap) was always followed by an increase in drag coefficient, and after tail slap the value of the drag coefficient fluctuated. Between tail slap and a distance of 50 calibers from entry, 80% of the instantaneous drag coefficients were between 0.28 and 0.40. The maximum and minimum coefficients measured during this portion of the trajectories were 0.48 and 0.23, respectively. The steady state drag coefficients measured within a range of cavitation numbers producing somewhat comparable cavities varied from 0.30 to 0.49[8] and, hence, are in fair agreement with the transient values obtained. Beyond a distance of 50 calibers from entry the measured drag coefficients varied from 0.14 to 0.35. Unfortunately, it was not possible to establish the end of the cavity phase. However, the data do show that the cavity was still present after the first 50 calibers of underwater travel.

Figures 7 and 8 show the variation in drag coefficient with time from entry during six typical tests. Tail slap and the approximate orientation of the projectile in the cavity are indicated on the curves.

Effect of Initial Pitch

The path of the torpedo could be varied from broach to steep dive by changing the initial pitch. The values of the critical pitch which separate the upturning from diving trajectories are tabulated in Table II.

When the torpedo was launched with large initial pitch, either flat or steep, tail slap occurred as the afterbody crossed the surface of

*See Appendix I for description of Launching Tank and Data Analyzer.

*Extrapolation of pressure distribution data[7,8] gives 0.26 for the $(C_d)_0$ based upon the diameter of the hemisphere. This reduces to 0.22 for the torpedo because the diameter of the hemispherical nose is less than the maximum diameter of the torpedo upon which the drag coefficient of the torpedo was based.

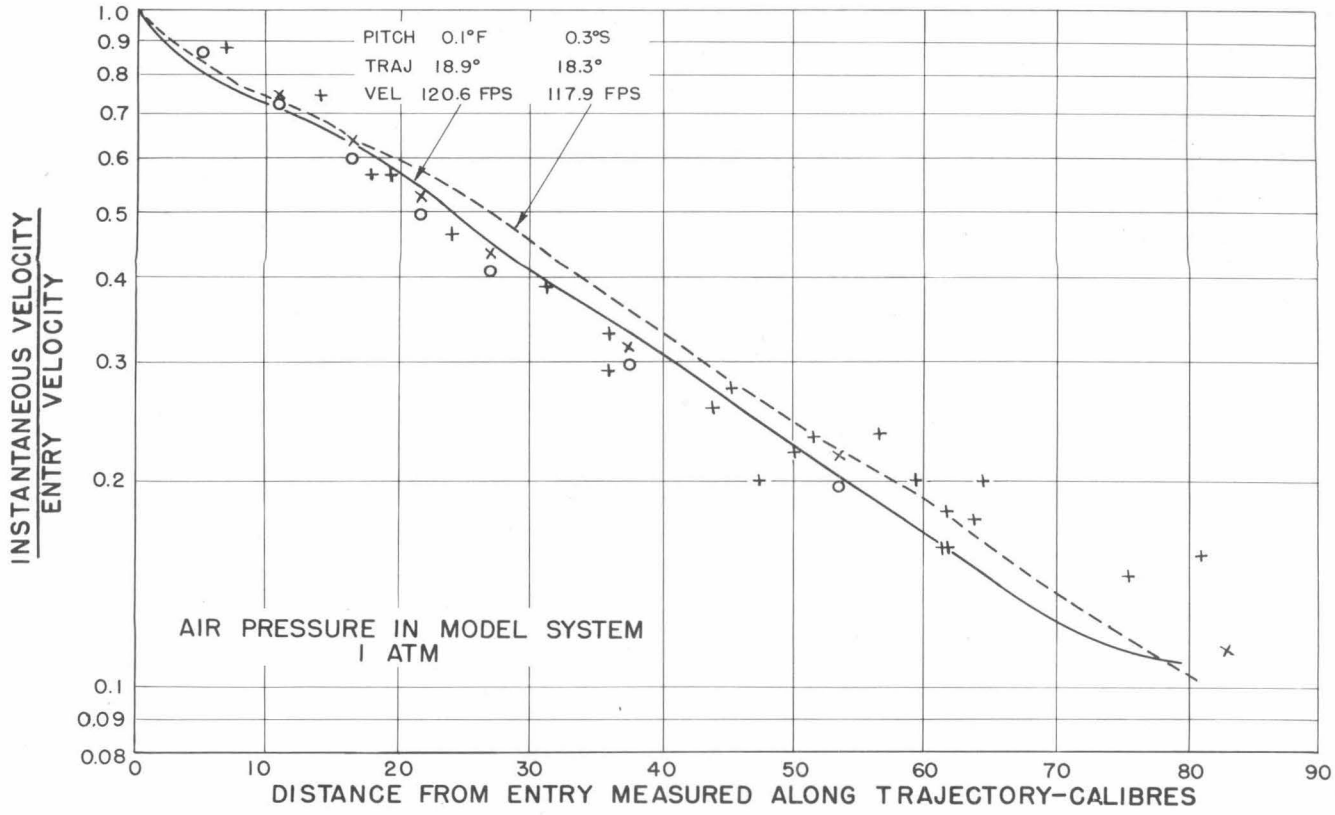

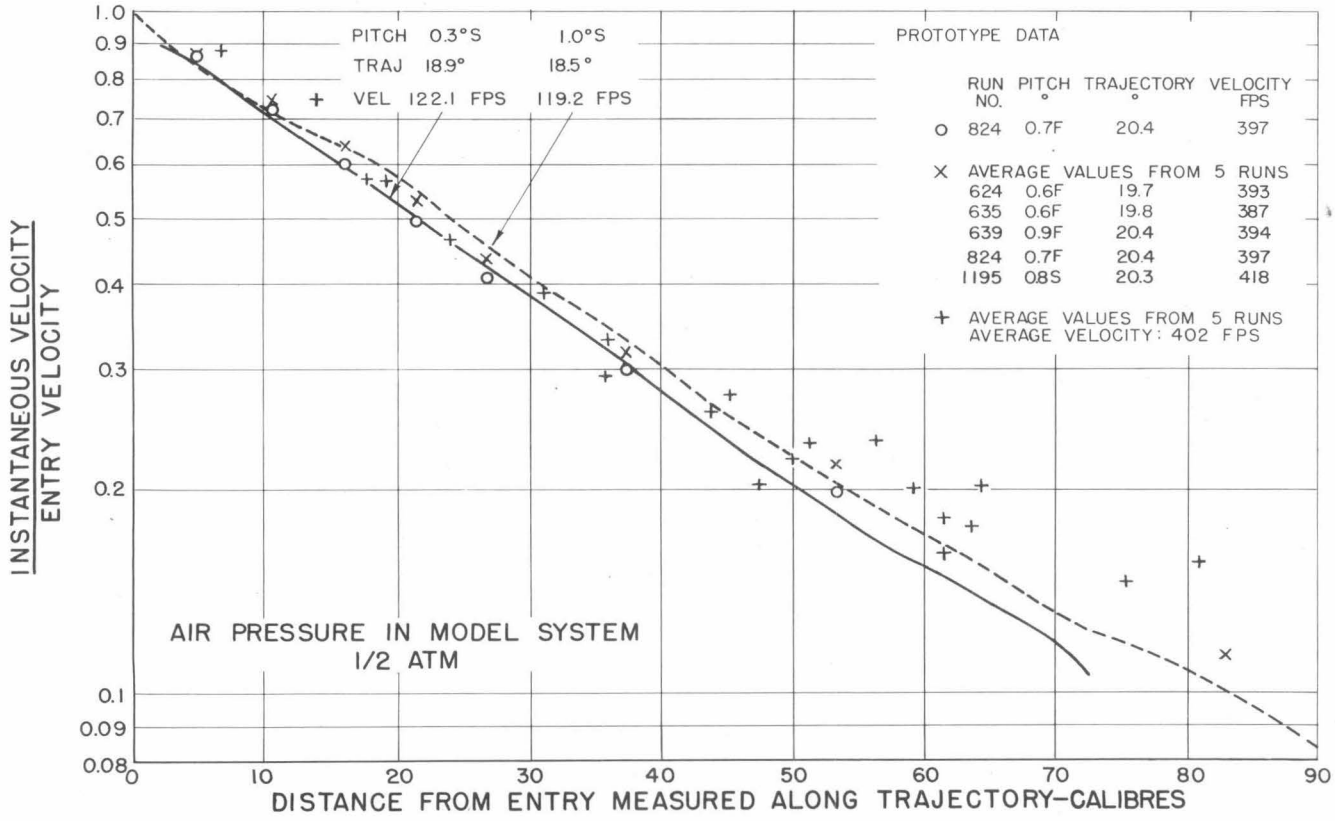

Fig. 3 - Velocity as a function of distance from entry measured along the trajectory for the standard Mk 13-6 torpedo model and prototype

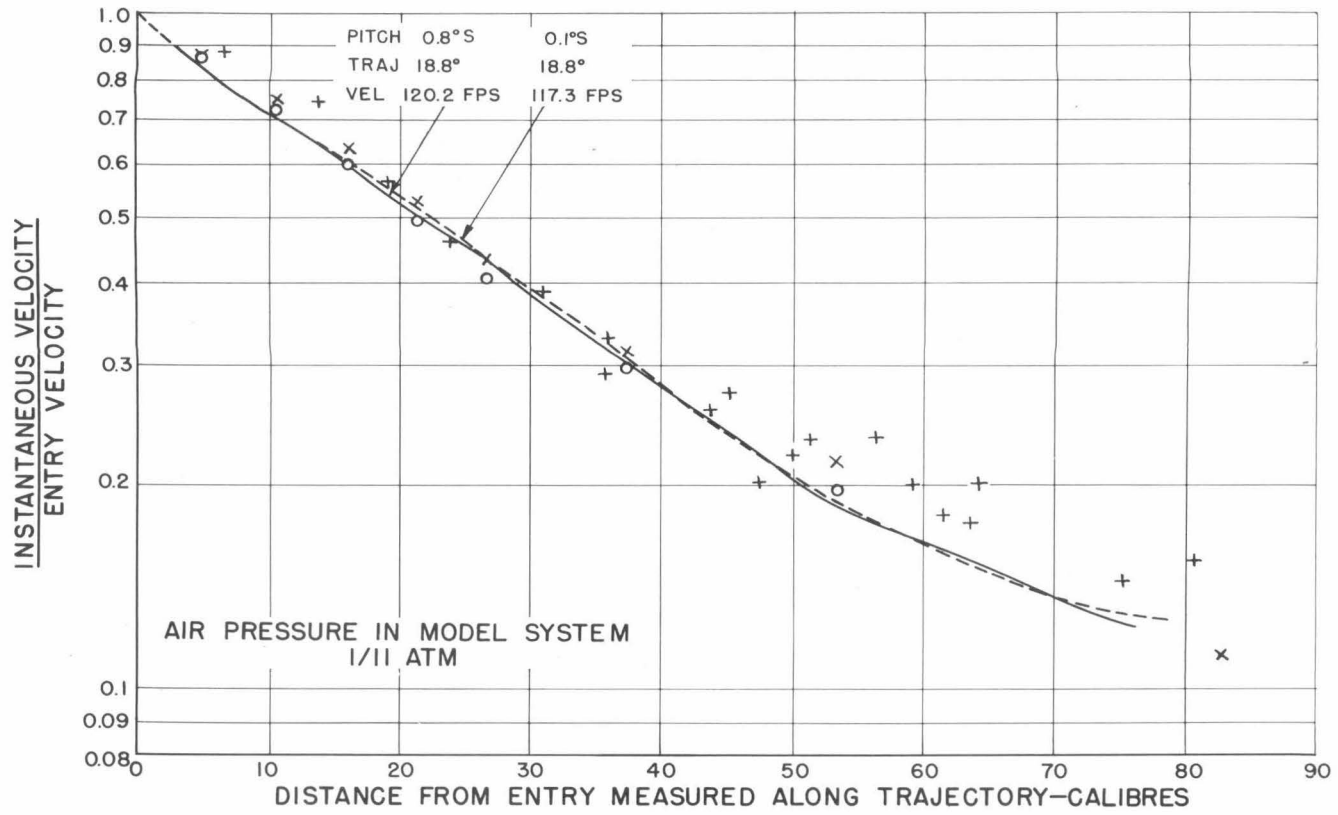

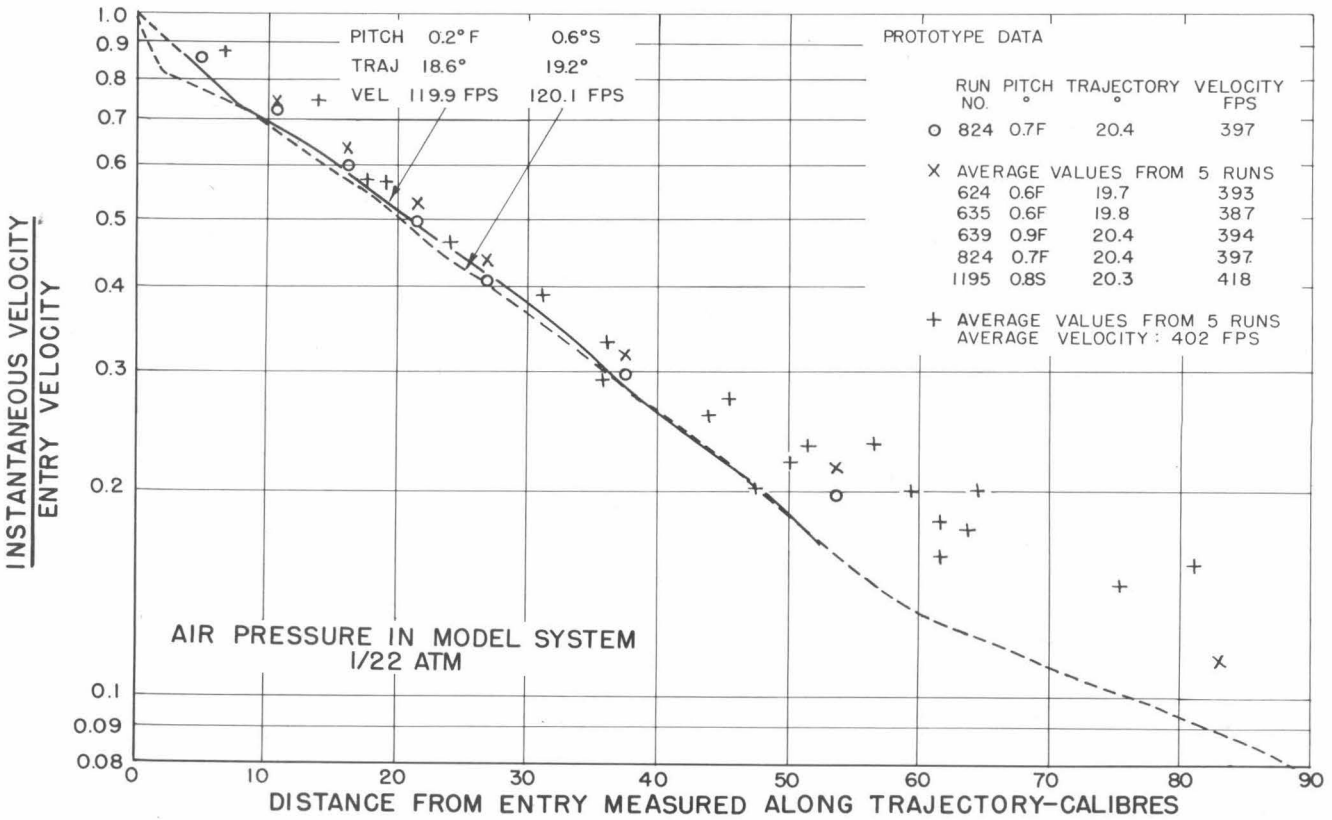

Fig. 4 - Velocity as a function of distance from entry measured along the trajectory for the standard Mk 13-6 torpedo model and prototype

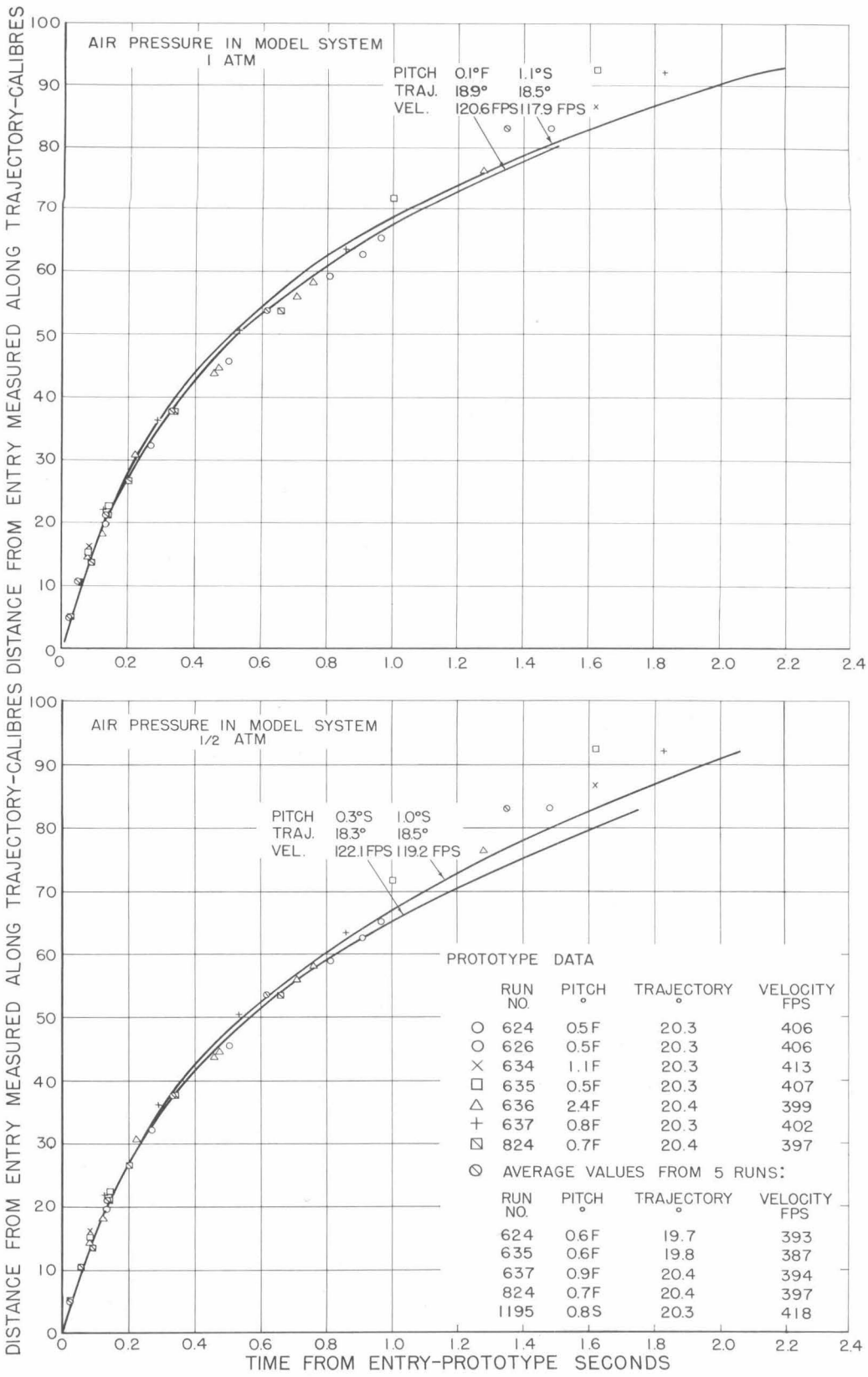

Fig. 5 - Distance from entry measured along the trajectory as a function of time for the standard Mk 13-6 torpedo model and prototype

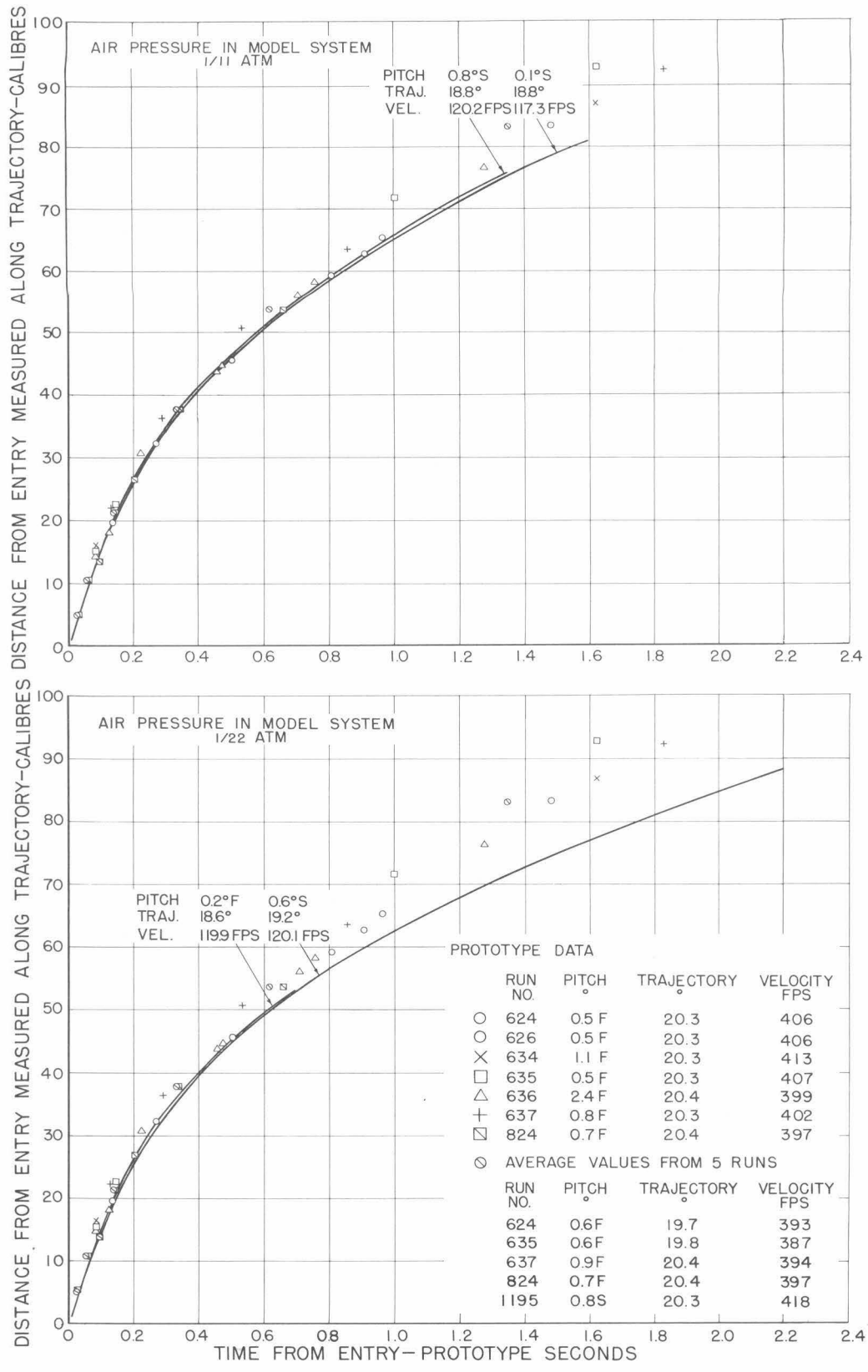

Fig. 6 - Distance from entry measured along the trajectory as a function of time for the standard Mk 13-6 torpedo model and prototype

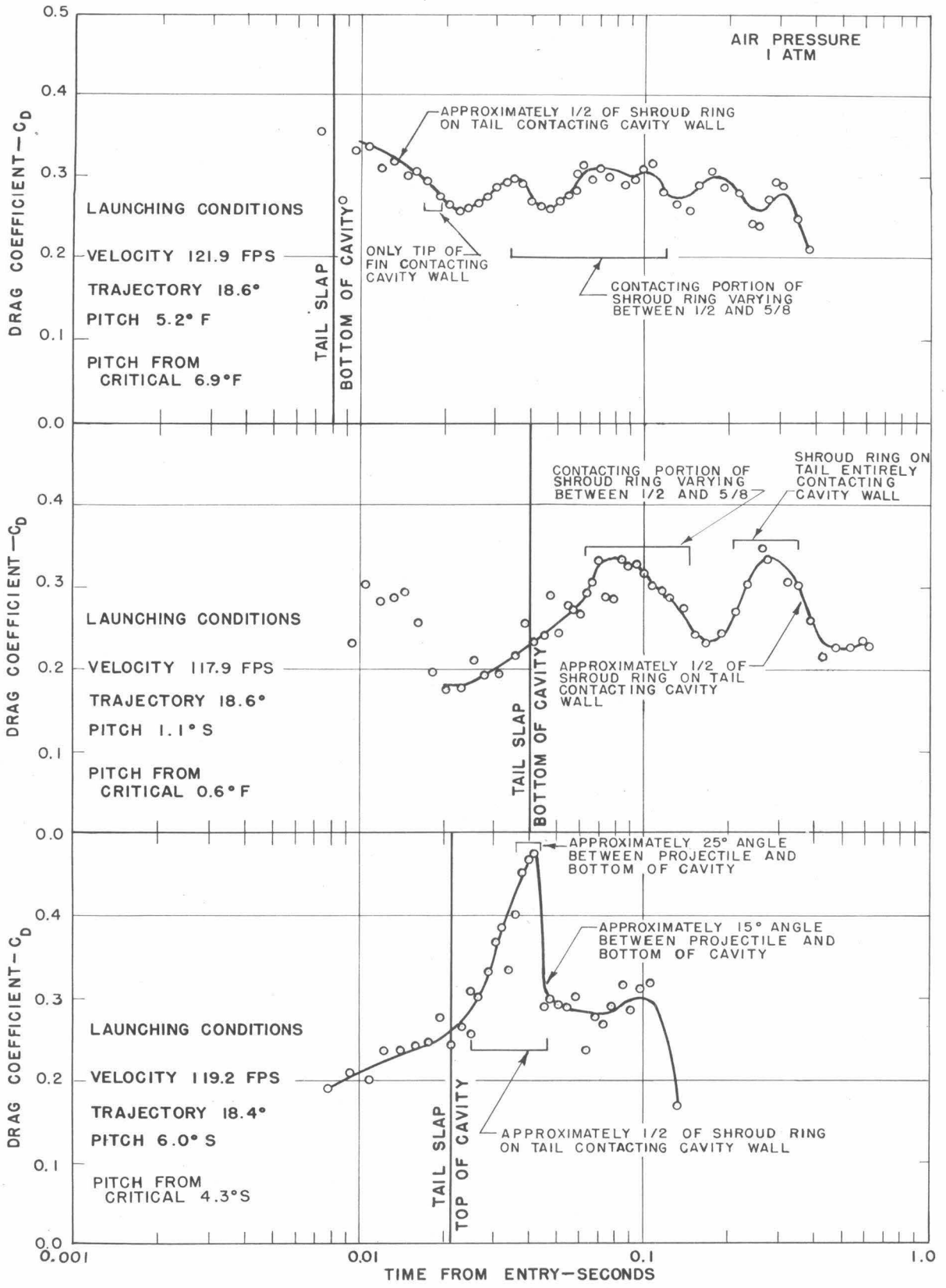

Fig. 7 - Instantaneous coefficient of drag as a function of time from entry for the standard Mk 13-6 torpedo model

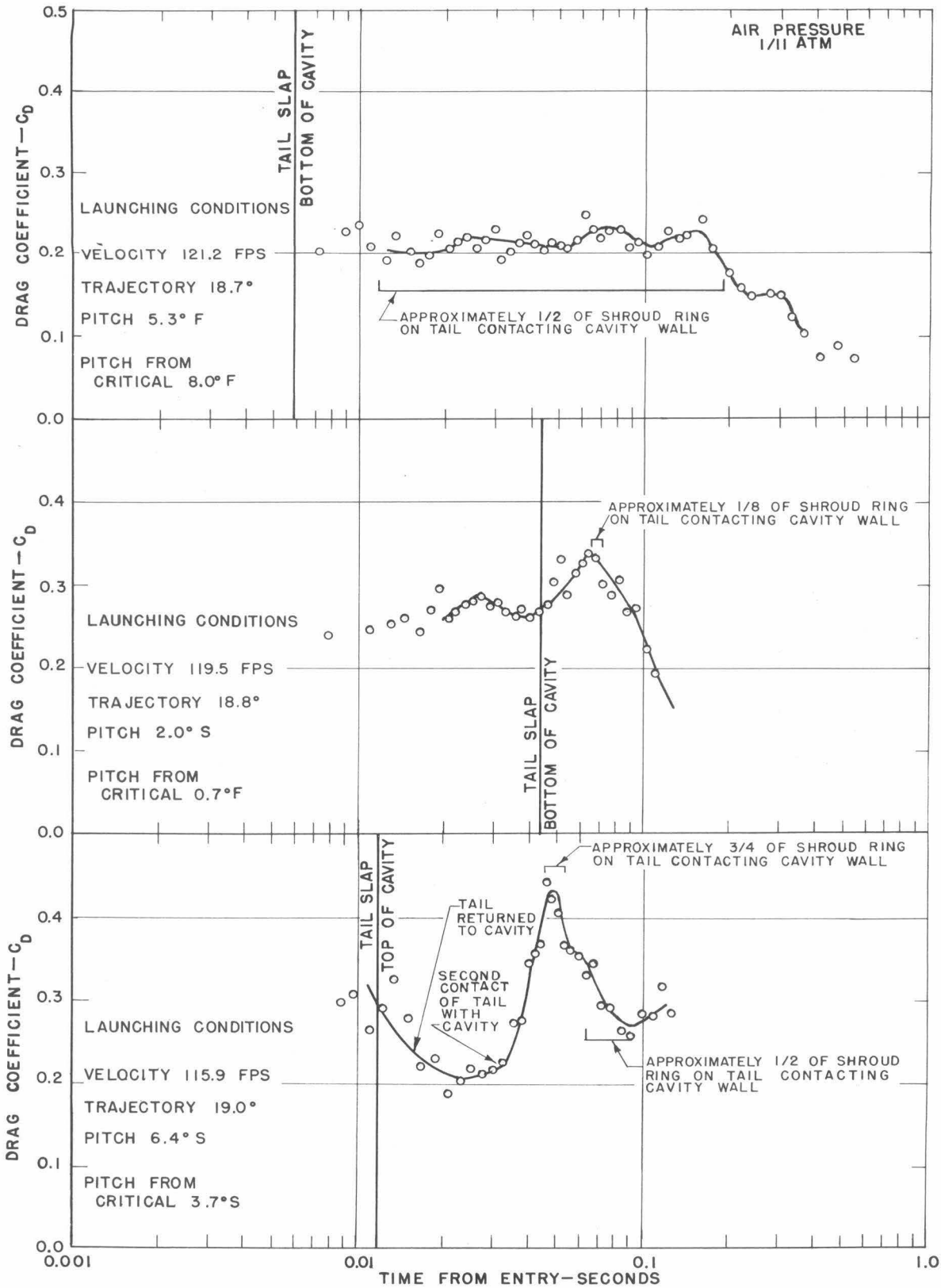

Fig. 8 - Instantaneous coefficient of drag as a function of time from entry for the standard Mk 13-6 torpedo model

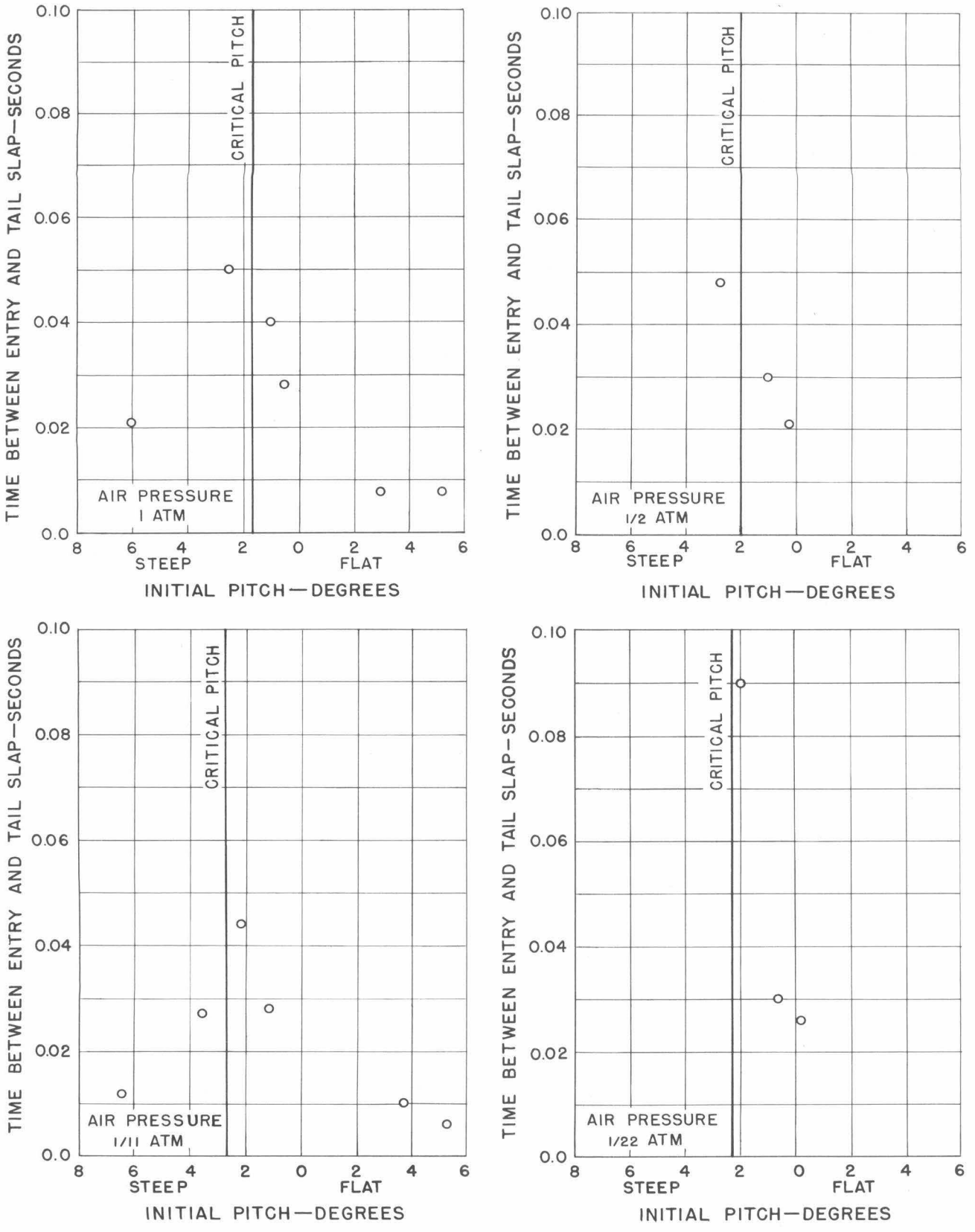

Fig. 9 - Time from entry to tail slap as a function of initial pitch for the standard Mk 13-6 torpedo model

the water. As the initial pitch approached critical pitch, tail slap became progressively later (Fig. 9). *If tail slap did not occur at entry*, the portion of the projectile in contact with the cavity wall after tail slap varied, causing the bubble configuration to fluctuate. At an initial pitch of about 0^{o} the entire shroud ring contacted the water at the cavity wall and then returned completely into the cavity. When tail slap occurred at entry, the orientation of the projectile in the cavity was relatively constant if the initial pitch was flat. If the initial pitch was steep, the orientation of the projectile was less stable. Since the torpedo contacts the top of the cavity when the initial pitch is steeper than critical, the lesser stability may be caused by the force of gravity pulling the projectile away from the cavity wall. Figures 10 and 11 include sets of drag coefficient vs. time curves from runs with air pressures of 1 atm. and 1/11 atm. arranged in order of increasingly steep initial pitch. Both the absolute initial pitches (pitch with respect to trajectory) and the initial pitches with respect to critical pitch are noted on these curves. The pitch with respect to critical should be used in comparing results from the two air pressures. These data show that the drag on the torpedo is similarly affected by change in initial pitch at both air pressures. Further, these data also show that the fluctuation of the instantaneous drag coefficient reflected the changing orientation of the projectile in the cavity. (Also see Figs. 7 and 8.) The drag coefficient was relatively constant after tail slap when the initial pitch was extremely flat. When the initial pitch was steeper than critical, the drag coefficient increased at tail slap and then diminished, suggesting that the projectile was falling away from the top of the cavity. At the intermediate initial pitches the drag coefficient fluctuated after tail slap, reflecting the bouncing motion of the projectile in the cavity.

The average drag on the projectile was perceptibly lower near critical pitch where the projectile traveled longest with only its nose in contact with the cavity wall. This is evident in Fig. 12, which shows the distance vs. time data taken with an air pressure of 1/11 atm. The curve from the run with an initial pitch close to critical is perceptibly higher than the others, indicating the lesser drag. The same effect was apparent at the other pressure conditions investigated.

Effect of Atmospheric Pressure

The standard Mk 13-6 torpedo is relatively insensitive to change in atmospheric pressure. However, some slight but consistent differences were noted. Within an initial pitch range of $\pm 1^{o}$, the average drag on the projectile during the first 75 calibers of travel increased slightly with decrease in atmospheric pressure.** This is evident from Fig. 13 which shows the distance vs. time curves from runs made at air pressures of 1, 1/2, 1/11, and 1/22 atm. The curves become progressively lower as the atmospheric pressure diminishes, indicating the increase in drag.

TABLE II. CRITICAL PITCH*
STANDARD Mk 13-6
TORPEDO MODEL

Tank Air Press. Std. Atm.	Critical Pitch o
1	1.7S
1/2	2.0S
1/11	2.7S
1/22	2.3S

*These values are from a pitch sensitivity study currently in progress in the launching tank.

The trajectories at 1/22 atm. differed somewhat in shape from those at the other pressures (Fig. 14). Further, the variation of mean drag as a function of time (or distance from entry) at 1/22 atm. differed from that at other pressures. At 1/22 atm. the mean drag coefficient increased with time (Fig. 15), while at the other pressures the mean coefficient remained essentially constant from tail slap to the end of the cavity phase.

Effect of a Finer Nose Shape on the Mk 13-6 Torpedo Model

Sensitivity to Atmospheric Pressure

The drag on the Head I model was lower than that of the standard Head F model. This is evident in Fig. 16, which shows the distance vs. time data from both the Head F and Head I torpedoes.

The instantaneous drag coefficients measured on the Head I model ranged from 0.10 to 0.38, (Fig. 17). The variation of instantaneous drag coefficient with time was similar for both torpedoes. Further, the mean drag coefficient of the Head I model increased with time only at 1/22 atm. (An increase in drag with decrease in pressure was also evident in the data taken with the Head F model.) However, the drag on the Head I model was extremely sensitive to change in atmospheric pressure, for the drag

**At the time of this analysis complete pressure-sensitivity data were not available for the extreme initial pitch conditions.

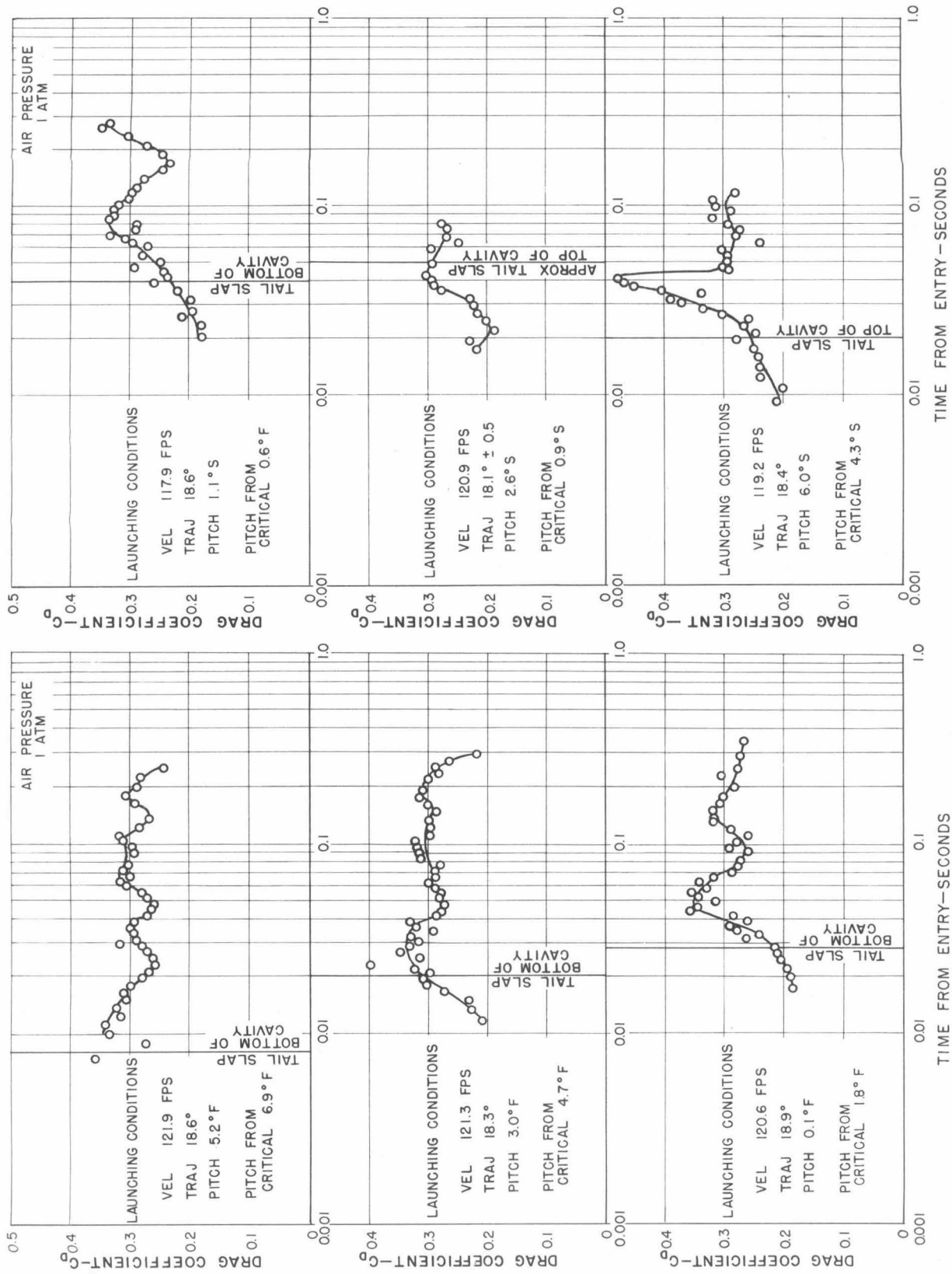

Fig. 10 - Instantaneous drag coefficient as a function of time from entry for the standard Mk 13-6 torpedo model

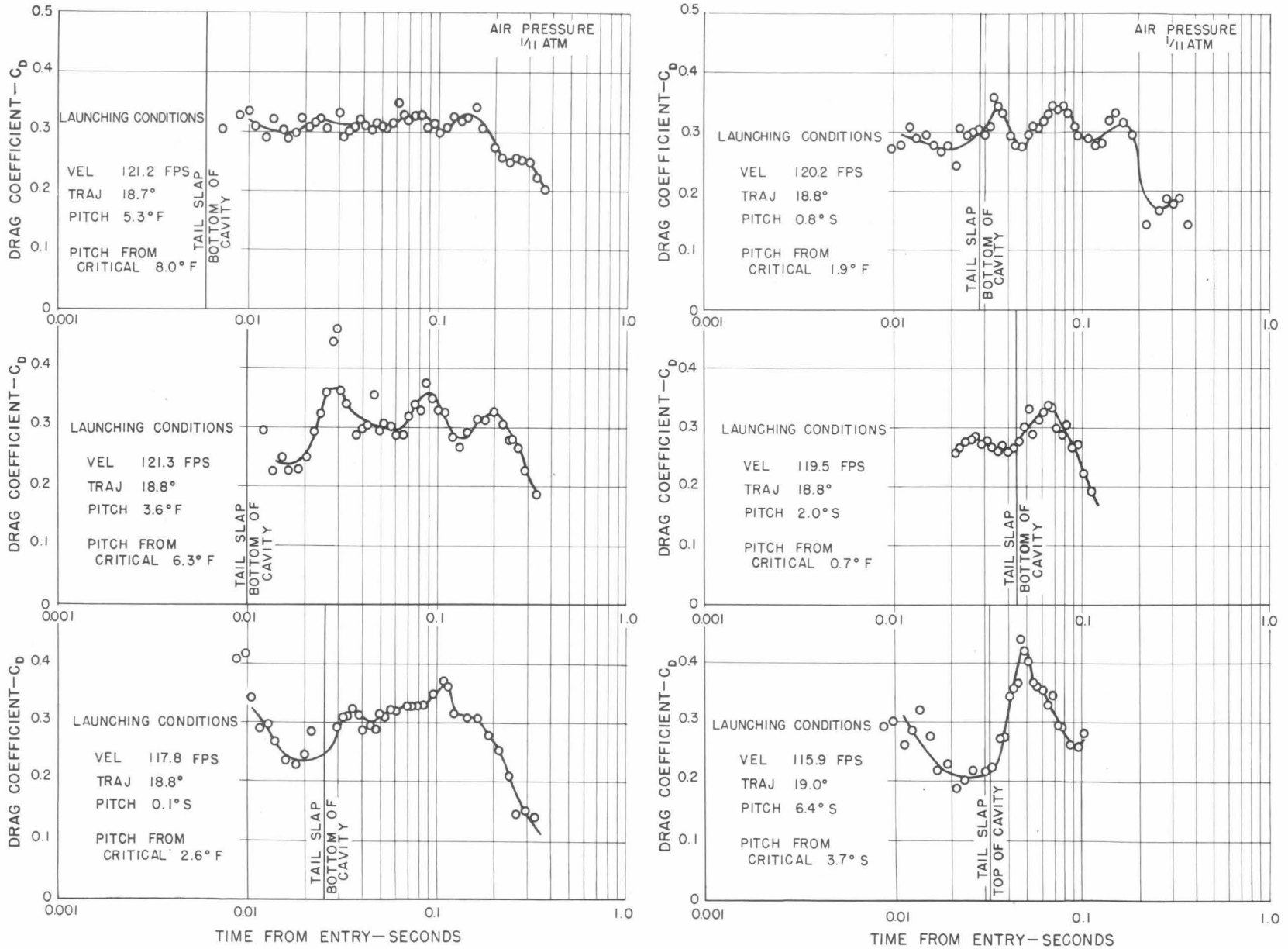

Fig. 11 - Instantaneous drag coefficient as a function of time from entry for the standard Mk 13-6 torpedo model

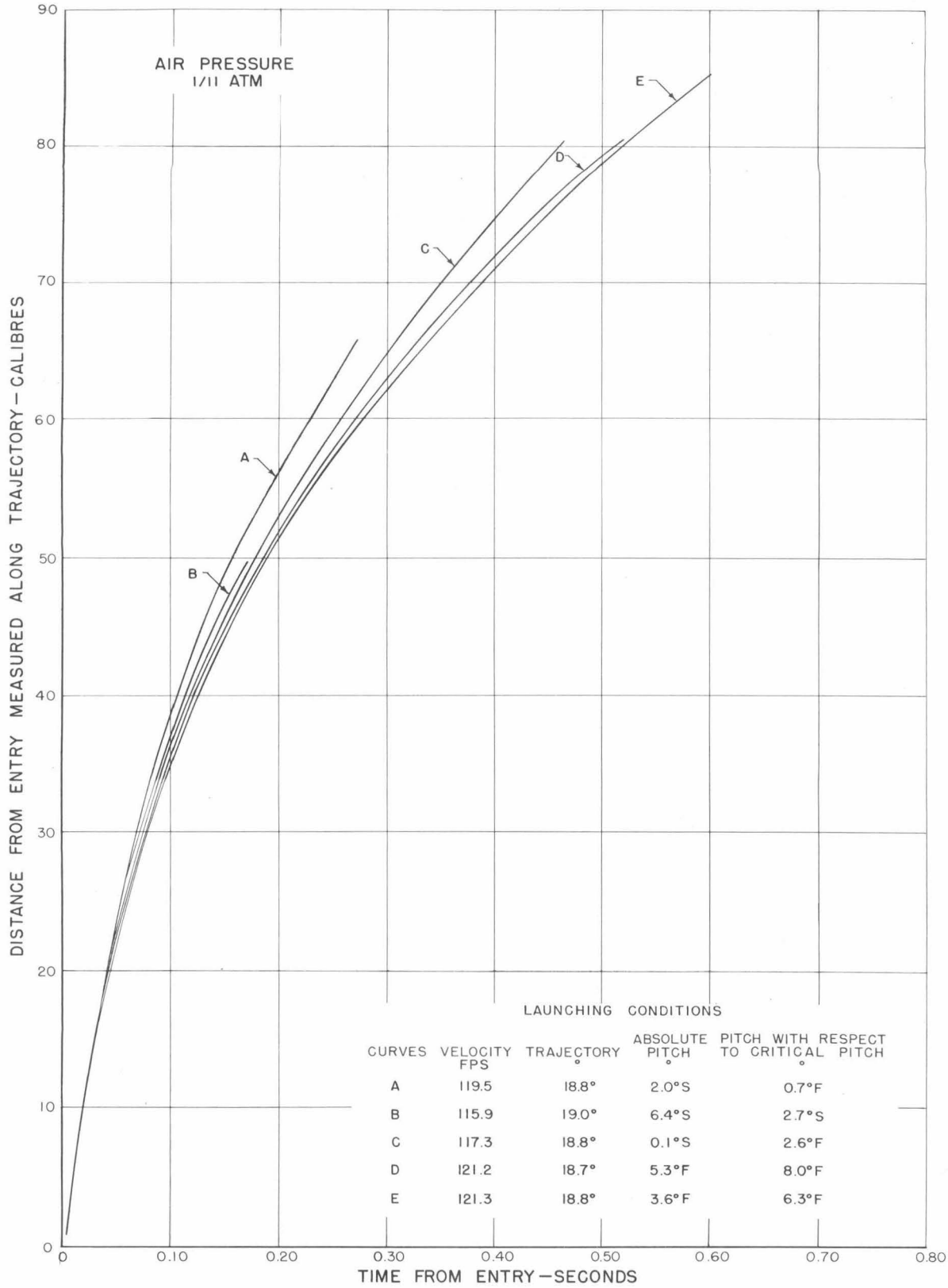

Fig. 12 - Distance from entry measured along trajectory as a function of time for the standard Mk 13-6 torpedo model

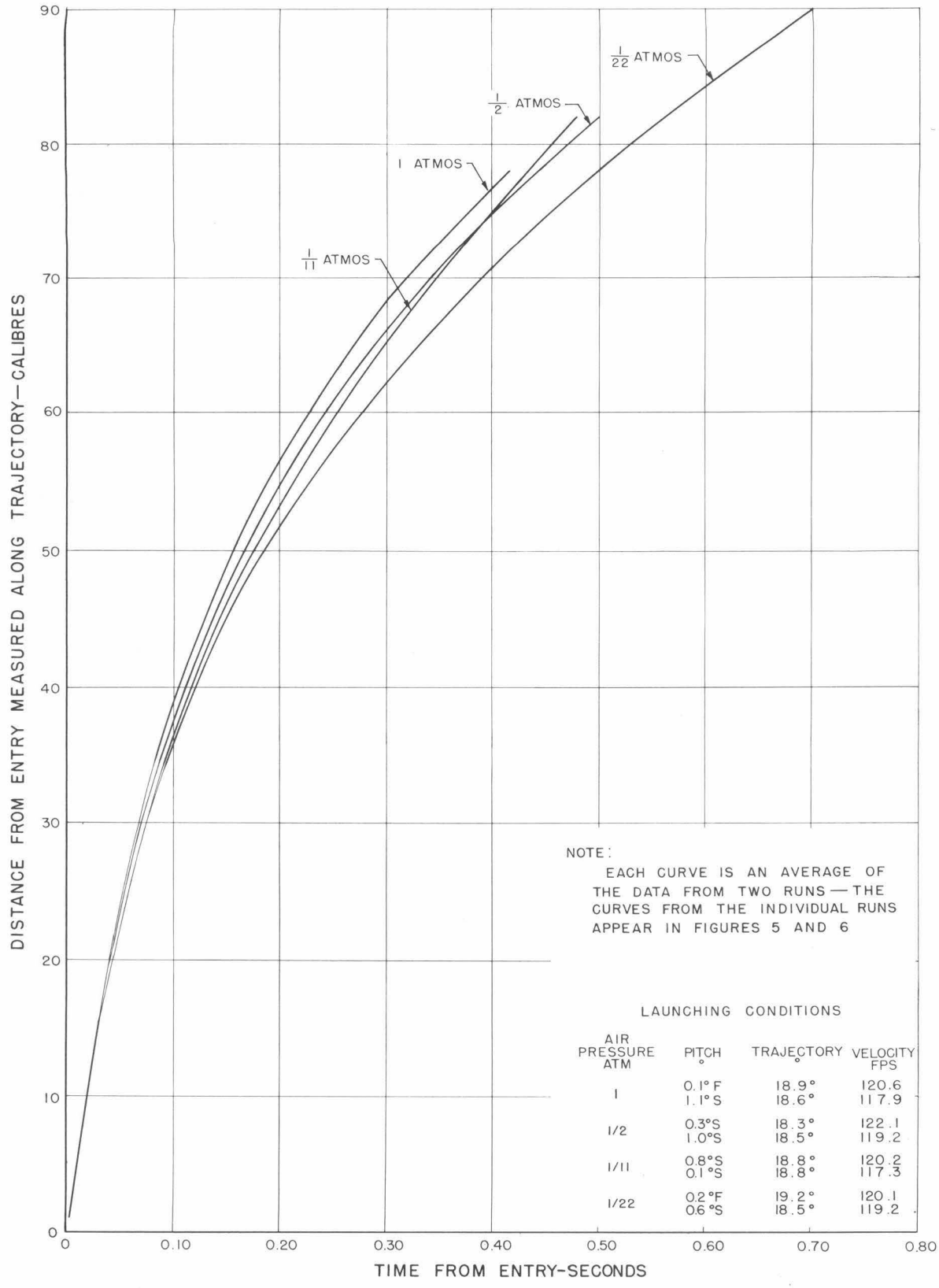

Fig. 13 - Distance from entry measured along the trajectory as a function of time for the standard Mk 13-6 torpedo model

coefficient increased about 80% when the air pressure was reduced from 1 atm. to 1/22 atm. This extreme sensitivity to pressure is not surprising because, as previously reported,[1] the trajectory of this model varied from a steep dive at an air pressure of 1 atm. to a broach at a pressure of 1/22 atm. The photographs in Fig. 18 were reproduced from actual test data recorded during the launching of the Head I model at an air pressure of 1 atm. The photographs show the instantaneous orientations of the projectile and the cavity at successive points along the trajectory.

Sensitivity to Initial Pitch

No pitch sensitivity data were available when this analysis was made. However, later visual observation indicated that the model with Head I behaved similarly to that with Head F. Its trajectory could be varied from broach to dive with change in initial pitch and the drag was slightly less near critical pitch.

Remarks

Further study of pressure-sensitive models is necessary to fully understand the markedly low drag on the Head I model at 1 atm. It is probably caused by the same phenomena which produce the steeply diving trajectory.[3] Unfortunately, the present data do not show enough of the cavity configuration to make measurement of the bubble diameter or determination of the separation point possible.

An extensive investigation of a shape that is pressure sensitive at model size is currently in progress. A wide range of carefully controlled conditions will be investigated with both model and prototype. From these data it is hoped to gain an insight of the physical conditions which produce the markedly low drag on the Head I model at 1 atm., and to determine conclusively whether a Froude-scaled, equal-cavitation number system will reproduce prototype drag characteristics.

CONCLUSIONS

The following conclusions were drawn from the results of this analysis:

1. Within an initial pitch range of $\pm 1^{\circ}$, the drag on the standard (Head F) Mk 13-6 torpedo during the first 50 calibers of underwater travel is modeled by Froude scaling to the accuracy of the prototype data. However, the results from runs made at 1/2 atm. and 1/11 atm. are in closest correspondence with the bulk of the prototype data.

2. Within an initial pitch range of $\pm 1^{\circ}$, the average drag on the Head F model during the first 75 calibers of underwater travel increases with decrease in atmospheric pressure.

3. The average drag on the Head F model is perceptibly lower near critical pitch.

4. The orientation of the Head F model in the cavity influences the instantaneous drag coefficient.

5. At a constant trajectory angle and entry velocity the initial orientation of the Head F model in the cavity is primarily determined by initial pitch.

6. The drag on the model decreases when the finer Dunn nose (Head I) is substituted for the standard Head F.

7. The Head I model is extremely sensitive to atmospheric pressure. The drag increases about 80% when the pressure is reduced from 1 to 1/22 atm.

8. The markedly low drag on the Head I model at 1 atm. and the phenomena causing it should be subjected to further study.

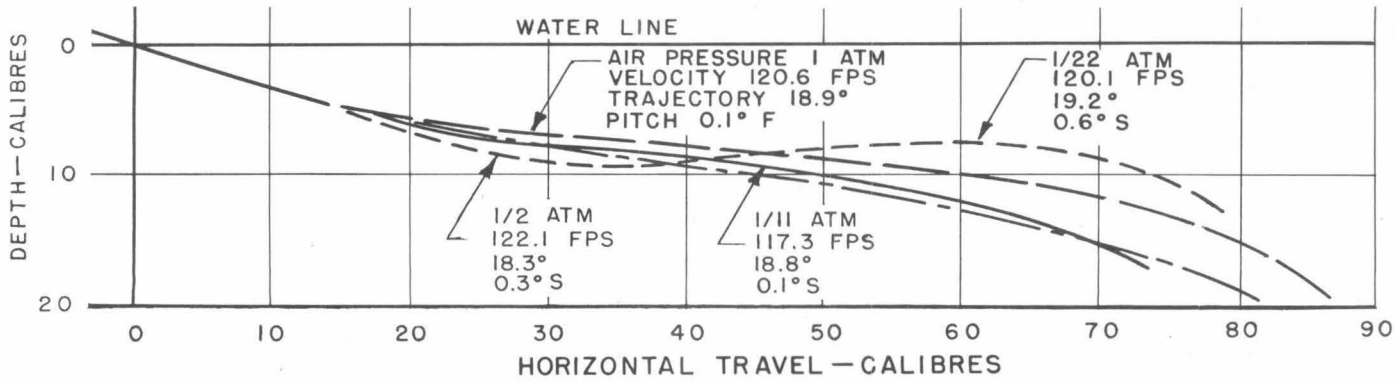

Fig. 14 - Effect of air pressure upon the trajectory of the standard Mk 13-6 torpedo model

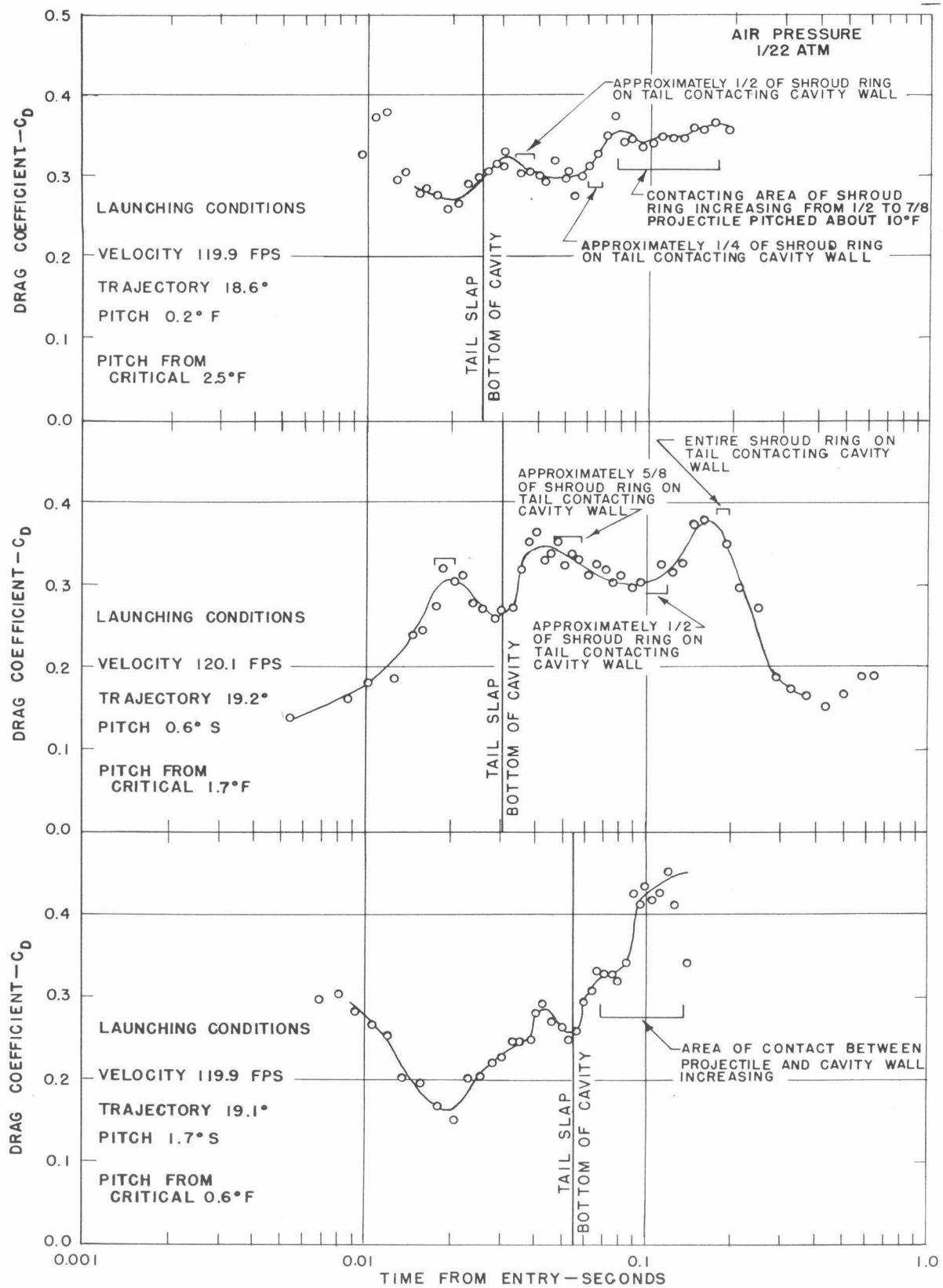

Fig. 15 - Instantaneous drag coefficient as a function of time from entry for the standard Mk 13-6 torpedo model

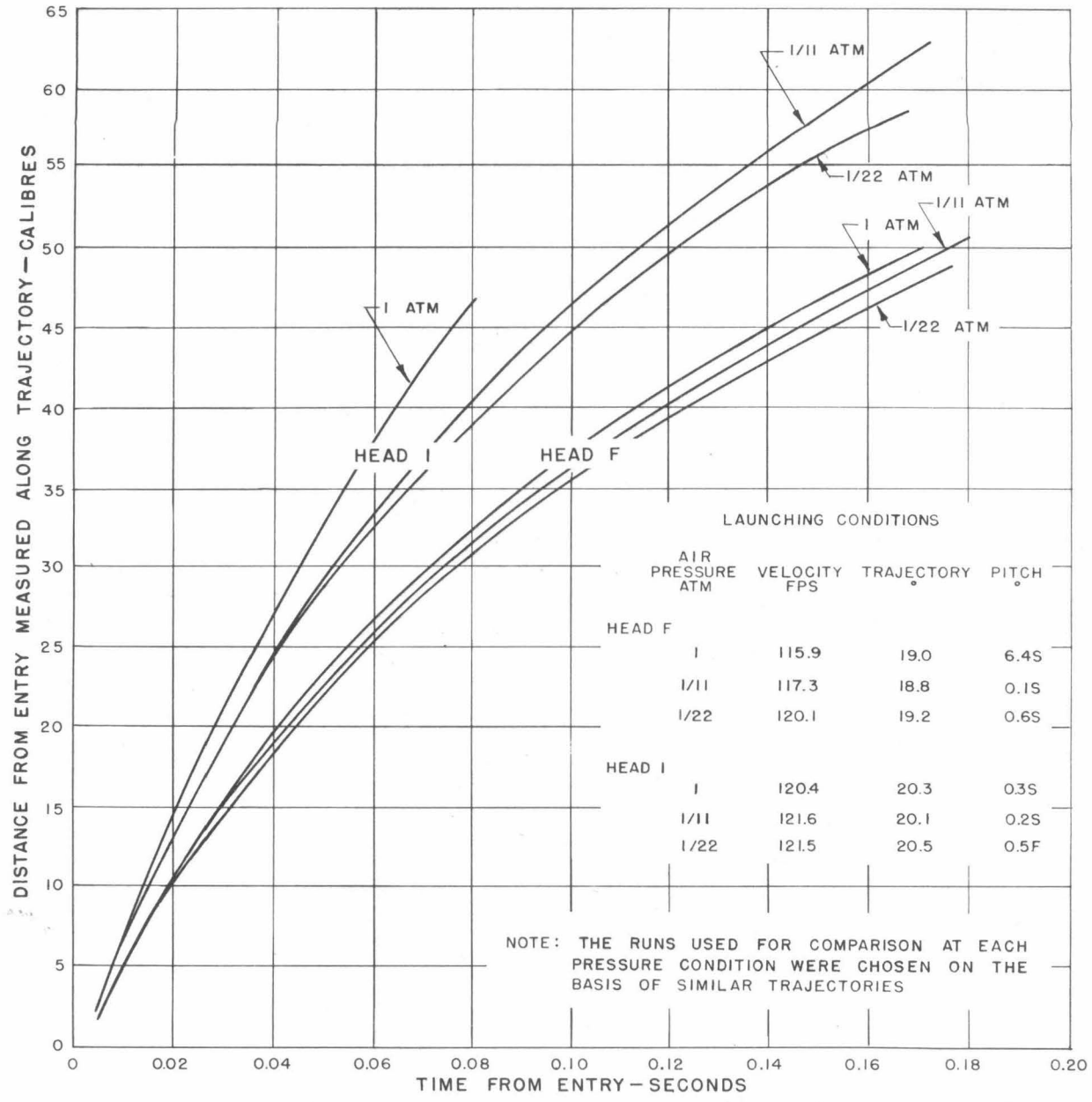

Fig. 16 - Distance from entry measured along the trajectory as a function of time for the standard (Head F) and Dunn (Head I) models of the Mk 13-6 torpedo

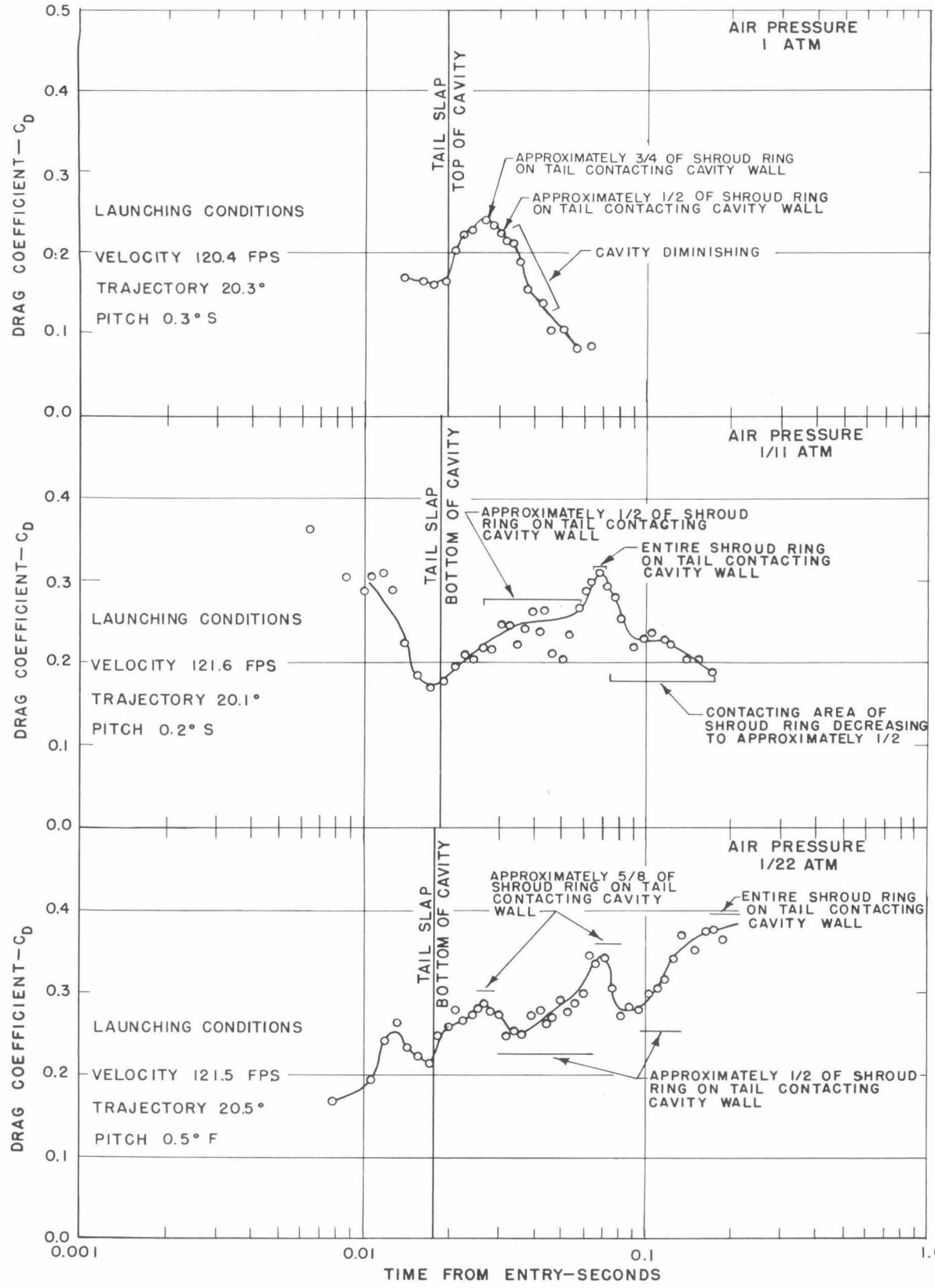

Fig. 17 - Instantaneous coefficient of drag as a function of time from entry for the Mk 13-6 torpedo model with the Dunn nose (Head I)

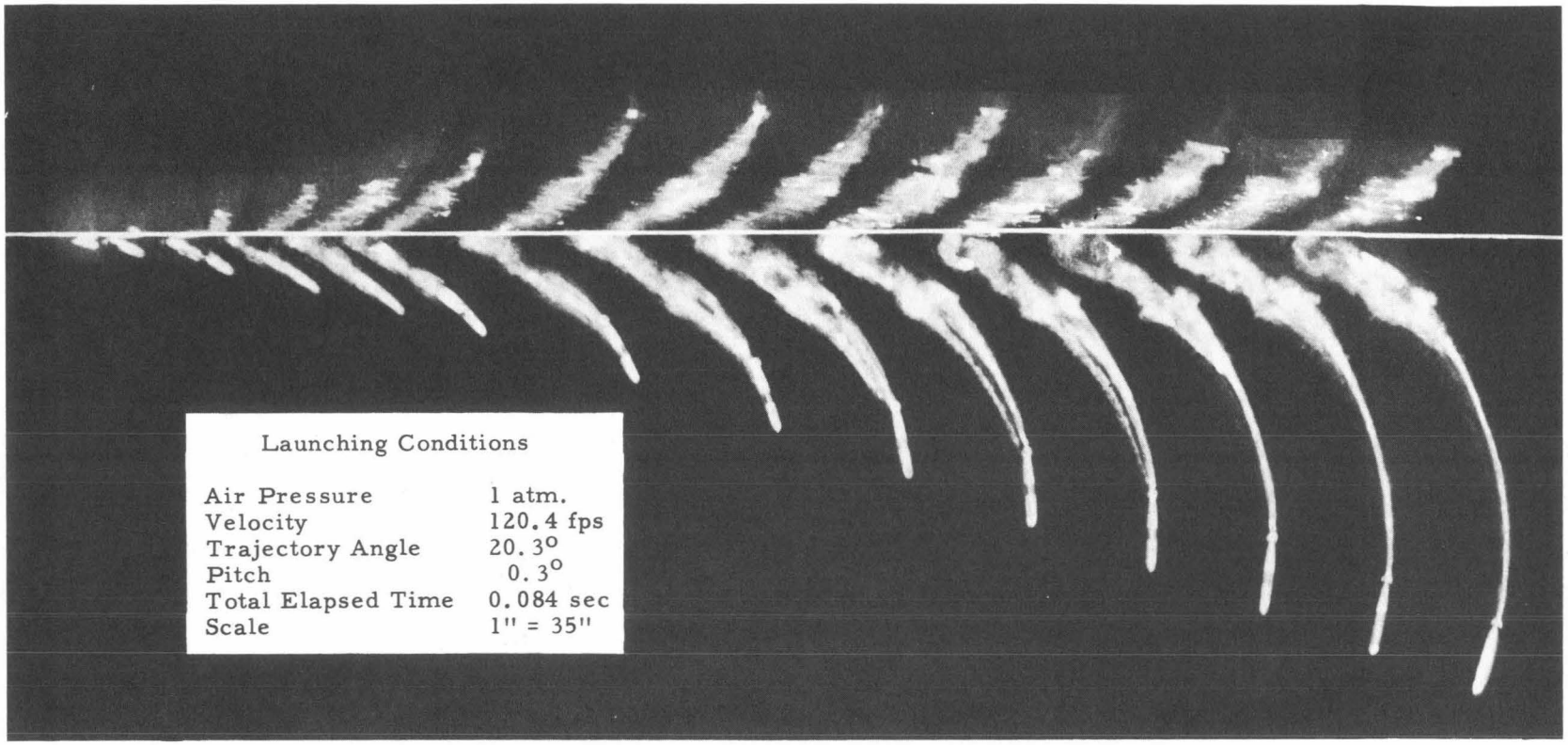

Fig. 18 - A steeply diving trajectory of the Mk 13-6 torpedo model with Dunn nose.

This composite photograph shows the instantaneous orientations of the projectile and cavity at successive points along the trajectory. The images above the horizontal line are reflections from the underside of the water surface.

Confidential

APPENDIX I

Apparatus

The Controlled Atmosphere Launching Tank[9]

The launching tank was designed to study the hydrodynamic factors involved when a body traveling freely through a gas strikes and penetrates a liquid surface. The tank provides control of launching velocity, pitch angle, trajectory angle and atmospheric pressure.

The tank is a Koroseal lined, welded steel pressure vessel 13 ft in diameter and 30 ft long with a smaller cylindrical bulge on one side (Fig. 19). The launcher, which is of the centrifugal type, is mounted on the underside of a large hatch cover on top of the tank. The model, held in a chuck near the periphery of the wheel, can be launched at any desired speed up to 120 fps at any angle between horizontal and vertical. The angle of the model with respect to the selected path can be adjusted to any angle up to $\pm 10^{o}$.

During normal operation the water is about 10 ft deep. The water is originally distilled and later maintained by constant filtration and ultraviolet radiation. These precautions are necessary because the underwater light path for photography is about 24 ft.

The path of the model through the gas above the surface of the water and under the water is recorded by two groups of high speed 35 mm. motion picture cameras operated at constant speed by a synchronous motor. The film is spliced to form one continuous loop in each camera magazine. In operation, the camera shaft is accelerated slowly to prevent film breakage. The cameras have no shutters. Exposures are made by intermittent illumination of the interior of the tank with Edgerton type flash lamps housed in lucite tubes located in the bulge of the tank. The number of exposures can be varied from 100 to 3,000 per second, and each flash is 2- to 3-millionths of a second in duration. The fields of view of adjacent cameras overlap to such an extent that the model is photographed by at least two of them during each exposure. This makes it possible to reproduce the path of the model by stereoscopic observation of the projected images.

The Trajectory Analyzer

The trajectory analyzer is a device for reconstructing the path of a model from the high-speed motion picture records obtained in the launching tank (Fig. 20). It provides information on the three linear and two angular components of position.

The analyzer is essentially a half-size reproduction of the recording system with projectors taking the place of cameras and a half model on a movable screen replacing the model. The screen can be moved to any position that the model may assume. The components of motion are indicated by counters which supply numerical trajectory data for further analysis.

All of the films from one run can be placed in the projectors with the film strips synchronized so that all frames taken simultaneously are projected simultaneously. A common drive operates the projectors so that the film strips remain synchronized during the projection of the entire run. For each frame the screen is maneuvered until the image falls on it. The counter readings give the position and orientation of the model.

Each projector (Fig. 21) is equipped with a lens matched with the corresponding camera lens. The gate mechanism holds the film exactly in the focal plane. Temperature changes in the projector are kept low by use of low light intensity, a water cell between the light and the condensers, and a small cooling fan.

Models

The models used in the launching tank are made in three sections which are connected by screw type joints. The nose and the afterbody are of duraluminum, the center section and fins and shroud ring on the afterbody are of stainless steel. The center section is grooved for fastening in the launching chuck. The groove should have little effect on the trajectory during the cavity stage, although it may have some effect later. The internal construction of the standard Mk 13-6 torpedo model is shown in Fig. 22. The Head I model is of similar construction. Figure 23 shows the outlines of both torpedoes with the external dimensions given in calibers, and Fig. 24 shows the outlines of the two noses superimposed for comparison.

The physical and dynamic characteristics of the models are listed in Table III together with the prototype dimensions and the correlation tolerances. The contours of the heads and afterbodies of these models were machined undersize to allow for a coat of white lacquer about 0.002 in. thick.

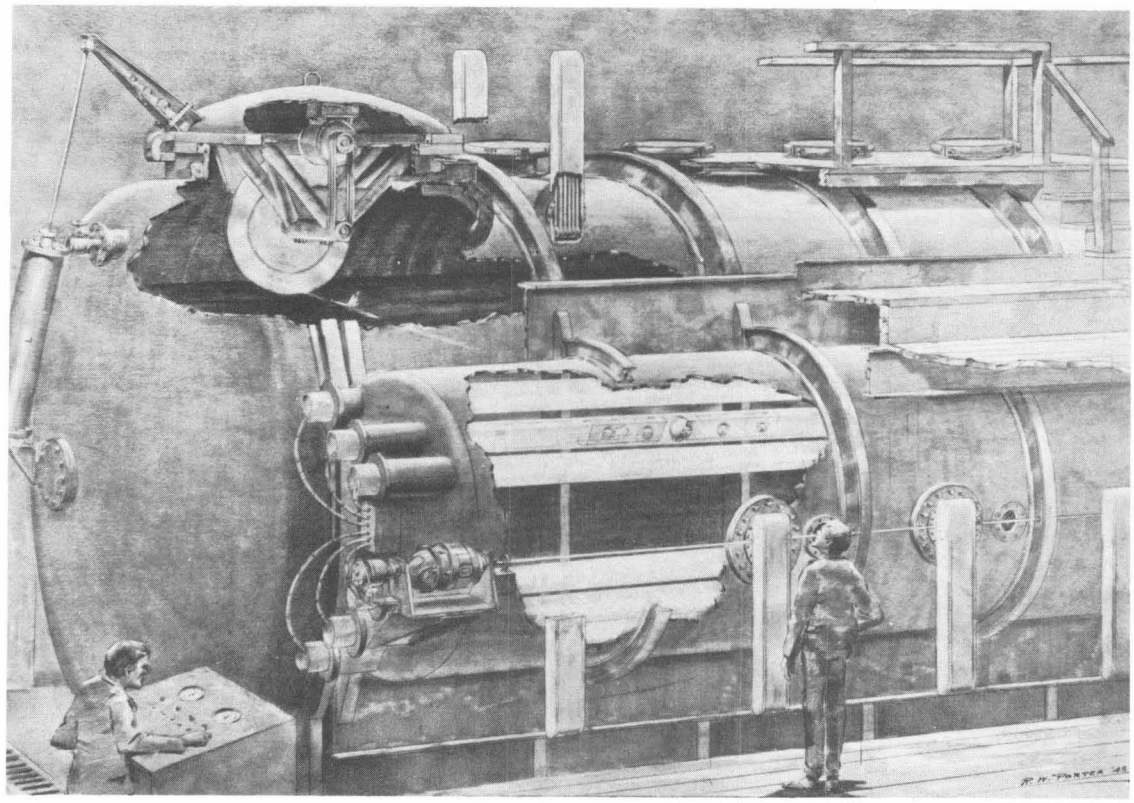

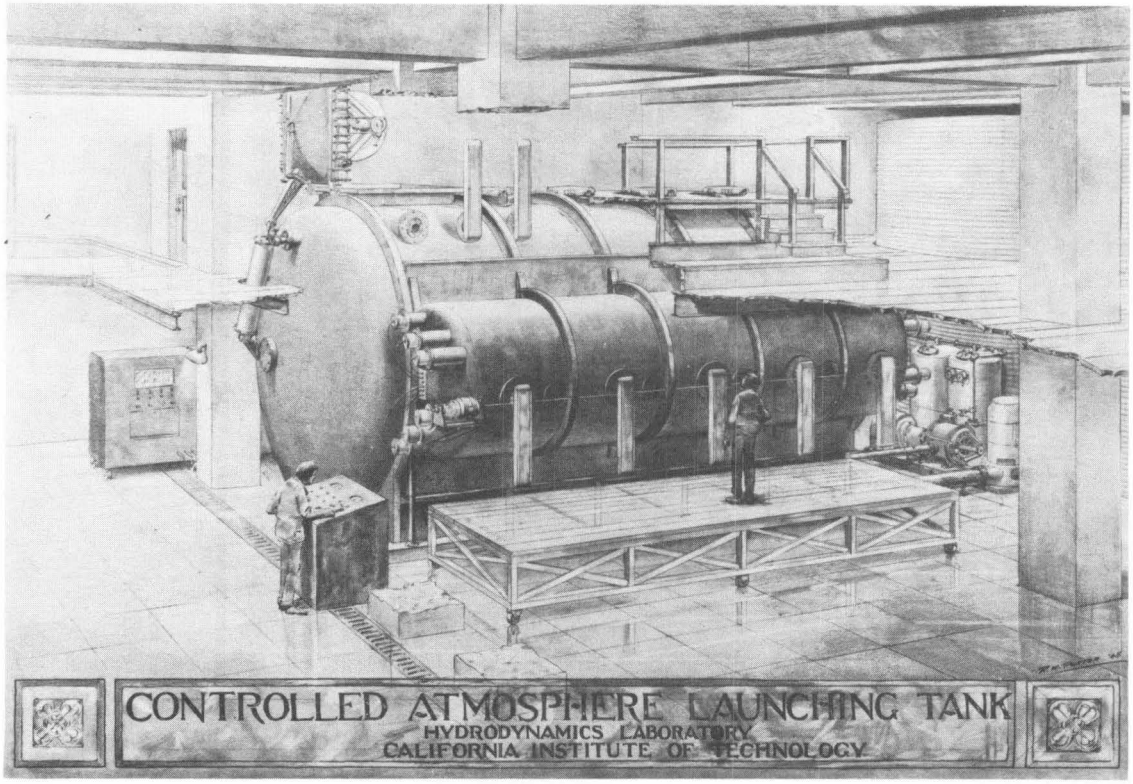

Fig. 19

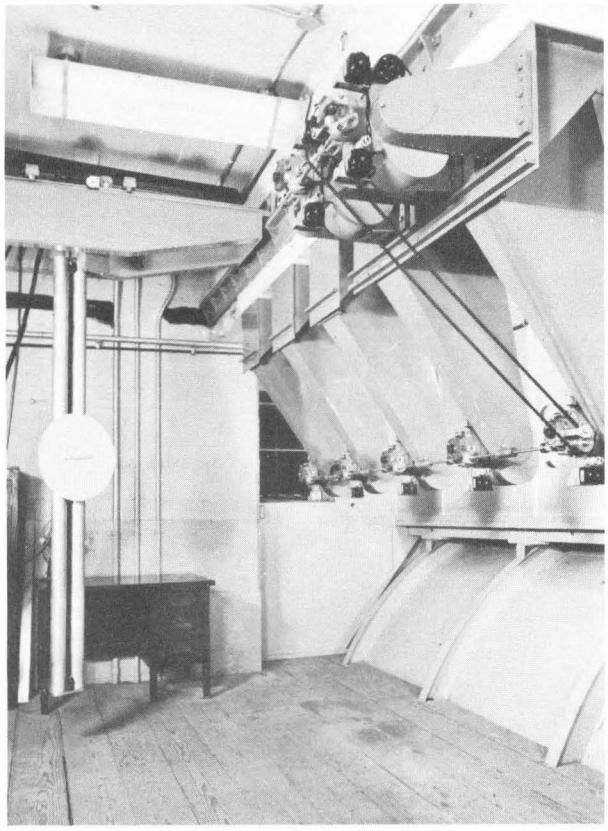

Fig. 20 - Trajectory analyzer

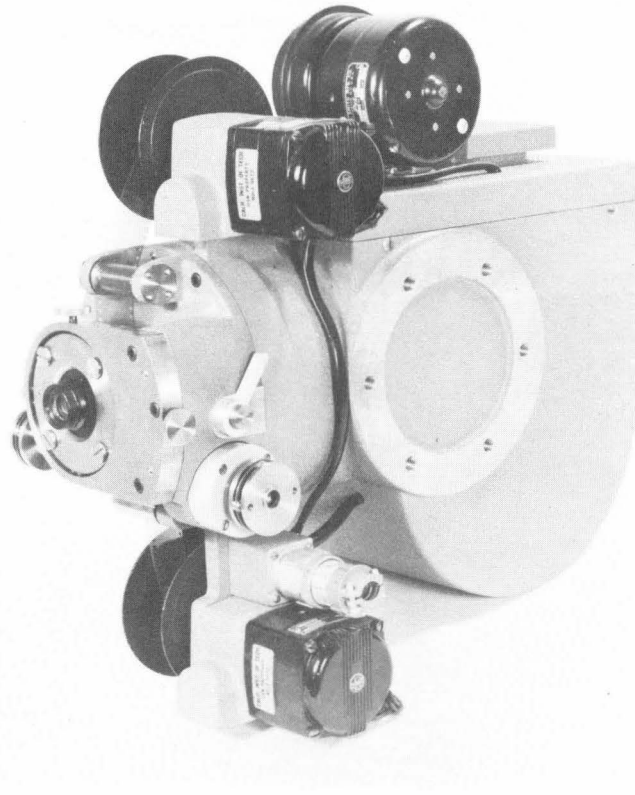

Fig. 21 - Close-up of projector

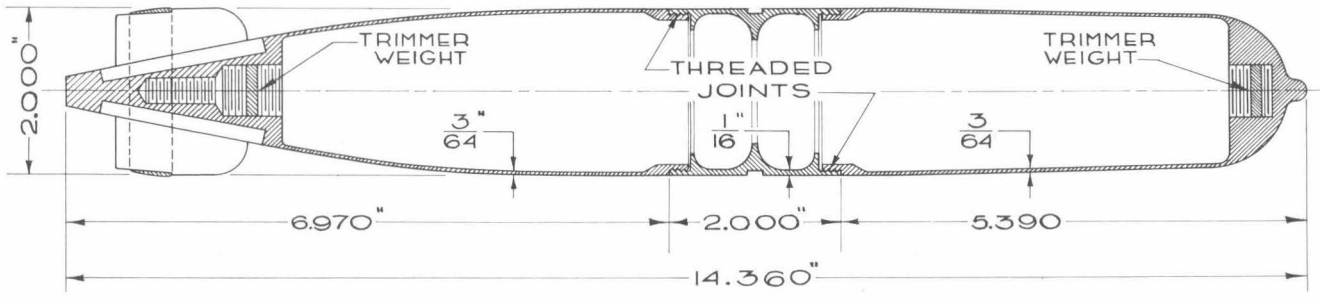

Fig. 22 - Sectional view of the standard (Head F) Mk 13-6 torpedo model

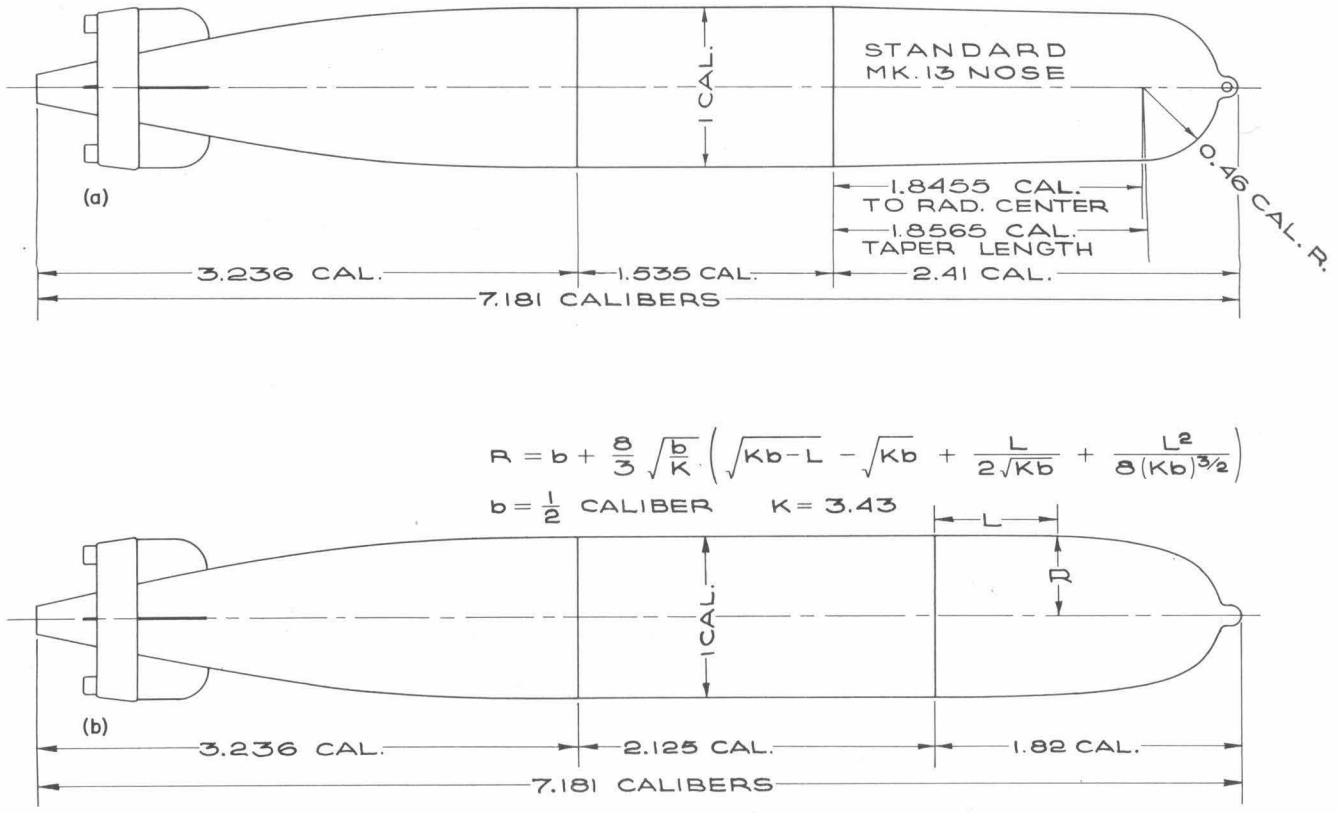

Fig. 23 - Outlines of the Mk 13-6 torpedo
(a) The standard (Head F) torpedo
(b) The torpedo with the finer Dunn (Head I) nose

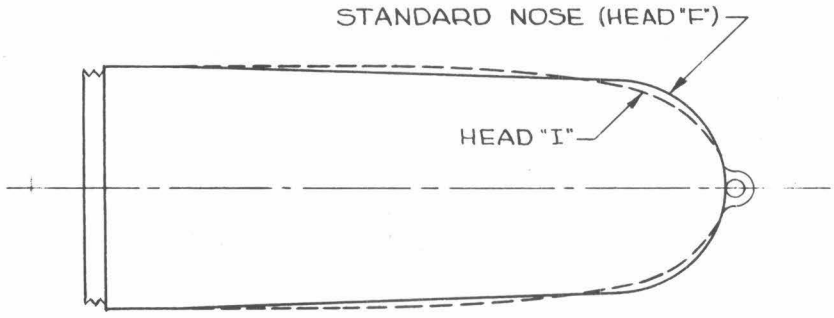

Fig. 24 - Comparison of the Head F and Head I contours

TABLE III. SPECIFICATIONS FOR THE PRECISION Mk 13-6 TORPEDO

	Model	Prototype
Length Ratio = L $1/L$ $\sqrt{L}$ $1/\sqrt{L}$	2 .50000 1.4142 .7071	22.42 .04460 4.7343 .2112
Scale Factor = S $1/S$ $\sqrt{S}$ $1/\sqrt{S}$	11.2100 .08921 3.3481 .29868	1 1 1 1
Diameter	2.0000 in. ±0.0027	22.42 +0.020 −0.010
Length*	14.16 in. ±0.08	158.7 in. ±1.0
Total Weight	1.079 lb ±0.01	1,520 lb ±15
Fresh Water Displacement	1.233 lb ±0.01	1,737 lb ±15
Buoyancy	0.154 lb ±0.02	217 lb ±30
Distance of c.g. from Nose*	6.178 in. ±0.04	69.25 in. ±0.50
Distance of c.b. from Nose*	6.234 ±0.04	69.88 in. ±0.50
Moment of Inertia about Transverse Axis through c.g.	0.1455 lb ft^2 ±0.0018	2.57×10^4 lb ft^2 $\pm 0.03 \times 10^4$

*Measured from tangent to hemisphere

APPENDIX II

Analysis of the Data

Reduction of the Photographic Data

The data used in this analysis were photographic records of launchings made in the Controlled Atmosphere Launching Tank. These photographs were taken at a rate of 500 exposures per second.

The film was analyzed to determine only the x and z coordinates of the model position and the inclination of the model axis with respect to the horizontal (Fig. 25). In some cases displacements occurred in the y direction during the water travel. However, the yaw was obvious from the divergence of data from adjacent cameras. Therefore, any data with sufficient yaw to affect the x and z coordinates were discarded. Coordinate positions were read to the nearest ± 0.01 diameter with an accuracy of ± 0.05 diameter in most cases and to ± 0.1 under the worst conditions. The experimentally determined trajectory angles are correct to ± 0.2°. During the air trajectory the inclination of the model with respect to the horizontal is correct to ± 0.1°. Since the initial pitch angle is the difference between the trajectory angle and the inclination of the model, the possible error in the initial pitch is ± 0.3°.

The Distance vs. Time Curves

The distance along the trajectory comes directly from the x and z coordinates measured with the analyzer.

The distance increment between any two

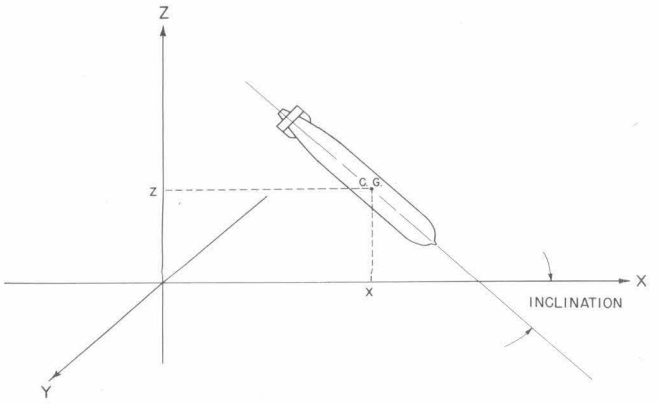

Fig. 25 - Coordinate system

points m and n along the trajectory:

$$s_{mn} = \left[(x_n - x_m)^2 + (z_n - z_m)^2 \right]^{1/2}$$

The total distance along the trajectory s_n at any point n is the sum of the individual distance increments from entry to point n:

$$S_n = \sum_{o}^{n} s_i$$

The intervals used were so small that approximating the curve of the trajectory within the interval with a straight line did not introduce appreciable error. The time t_n plotted with the distance S_n was measured by the accurately known flash rate of the lights. The sample distance vs. time curve (Fig. 26) shows that these data were virtually without scatter.

The frame designated as "one" in the original data was the frame in which the nose of the projectile first penetrated the water. The actual entry of the nose occurred somewhere between 0 and -0.002 sec. No attempt was made to correct for this.

The Velocity-Time Curves

The velocities came from the first differentiation of the numerical distance-time data:

$$v_n = \frac{S_n - S_m}{t_n - t_m}$$

Overlapping intervals were used in the early portion of the trajectory where conditions were changing rapidly. There was some scatter in the velocities, particularly at the extremes of the trajectory where the original data were less reliable. However, the sudden changes in velocity which resulted from tail slap and other changes in orientation could be separated from scatter in the data because the orientation of projectile and cavity were readily apparent in the original photographs. The times plotted with the v_n in Fig. 26 were determined by:

$$t_{avg} = \frac{t_m + t_n}{2}$$

The Coefficient of Drag

The coefficient of drag is proportional to the slope of the curve that results when the logarithm of the instantaneous velocity is plotted against the distance traveled from water entry. The force tangent to the trajectory can be written as:

$$F = \frac{mdv}{dt} = -\frac{C_d A \rho v^2}{2} + g(m - \rho V_w) \sin \theta \qquad \text{(See Fig. 27)} \qquad (1)$$

The gravity-buoyancy term $g(m - \rho V_w) \sin \theta$, significant only at the low velocities beyond the cavity phase, was not considered in either model or prototype work; nor was any virtual mass correction made. If the gravity-buoyancy term is dropped, Eq. (1) may be rearranged and integrated to give:

$$\ln v_1/v_2 = \frac{C_d A \rho (S_2 - S_1)}{2m} \qquad (2)$$

where S = distance from entry measured along the trajectory.

Whence:

$$C_d = \frac{2m \ln v_1/v_2}{A (S_2 - S_1)} = \frac{3.726 \log v_1/v_2}{(S_2 - S_1)} \qquad (3)$$

The velocity-distance curves used to calculate the drag coefficient were plotted from the faired velocity-time and distance-time curves. Figure 28 compares the velocity-distance curve from the faired velocity data with the points from actual computed velocities. Since the distance-time data are virtually without scatter, it is reasonable to assume that the velocity distance curves are not distorted in shape by the scatter in the velocity data.

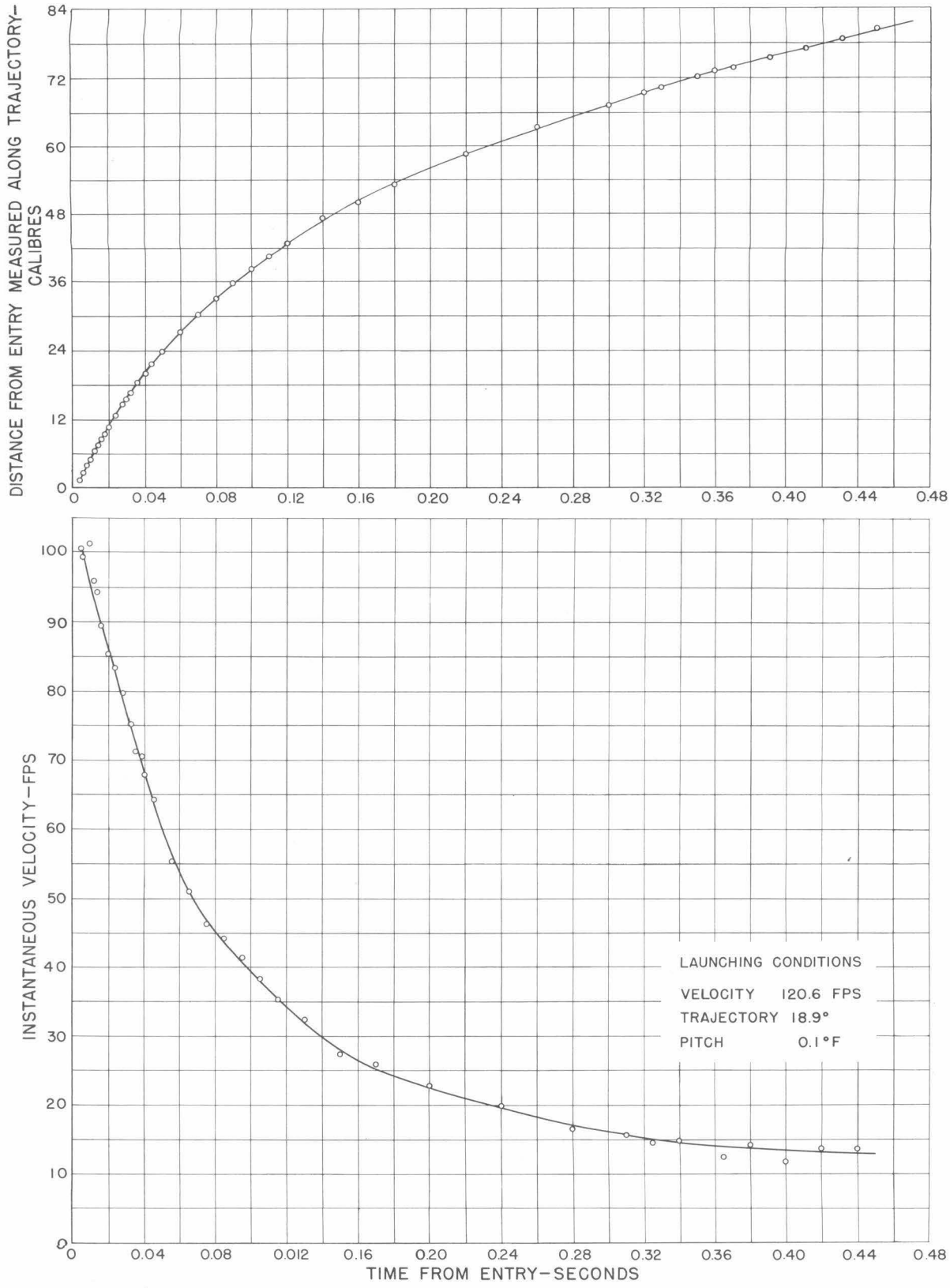

Fig. 26 - Distance from entry measured along the trajectory and instantaneous velocity as a function of time for the standard Mk 13-6 torpedo model

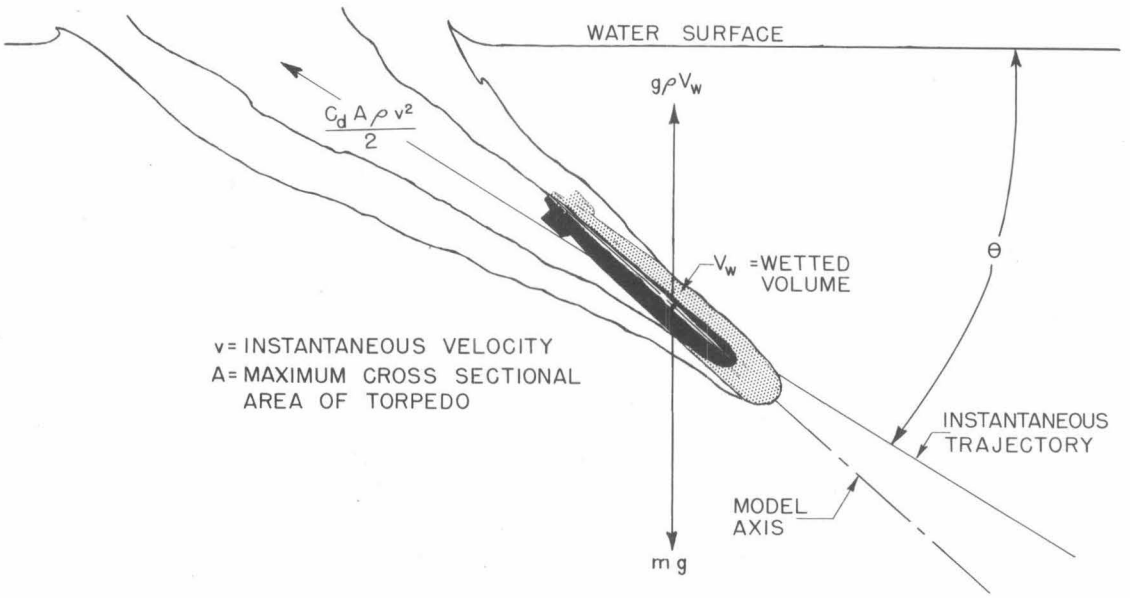

Fig. 27

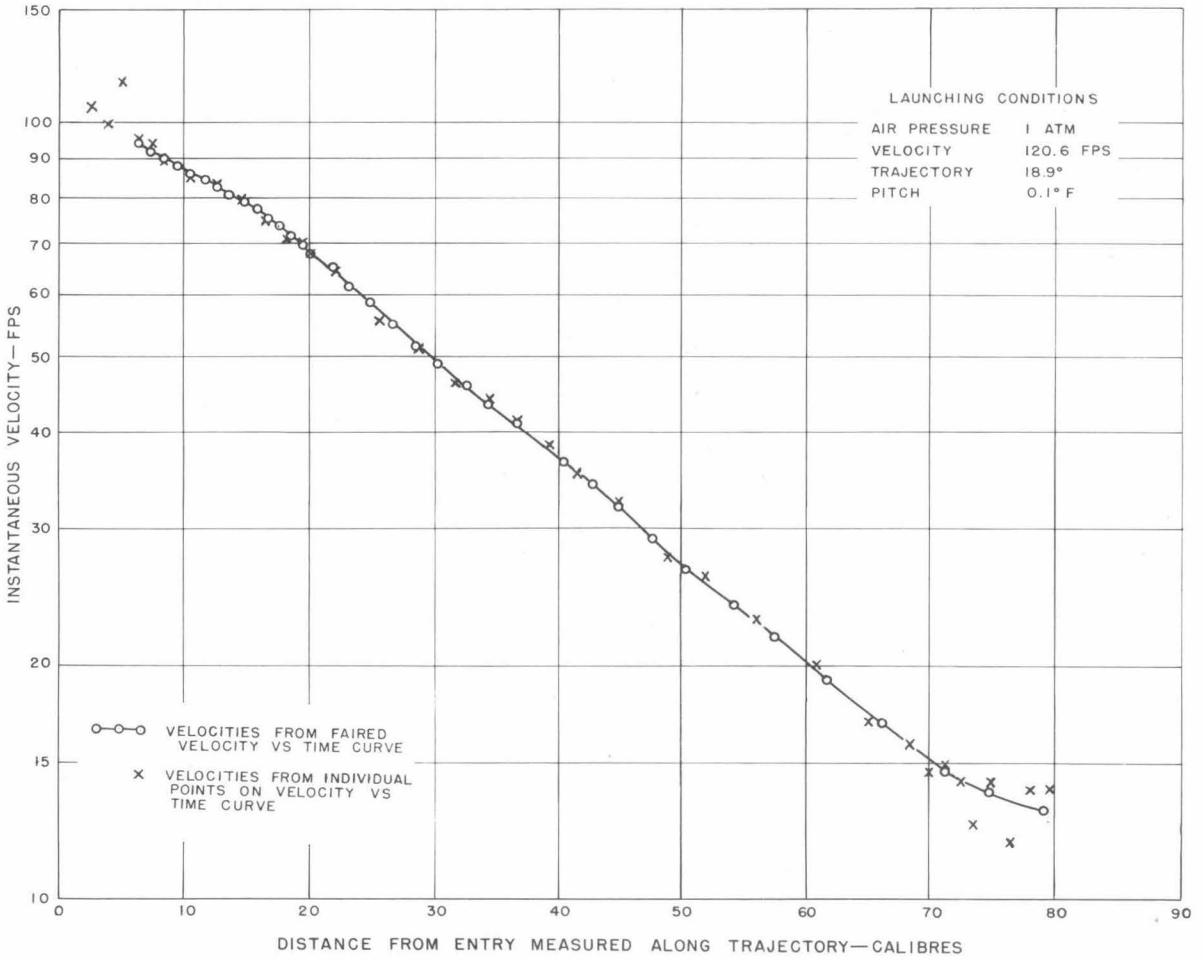

Fig. 28 - Instantaneous velocity as a function of distance from entry measured along the trajectory for the standard Mk 13-6 torpedo model

APPENDIX III

Factors in Model Studies of Water Entry

In studying the behavior of free-flying bodies by means of scale models, the aim is to control the variables which affect the motion so that the model will follow a path which is geometrically similar to that of the prototype and so that the scale ratio of the two paths will be the same as the ratio between the linear dimensions of the model and of the prototype. This requires that the pressure distribution on the model be similar to that on the prototype at corresponding points of the trajectories.

The phenomena associated with the water entry of an aircraft torpedo are complex. Since only a limited number of the contributing factors can be modeled simultaneously, it is necessary to consider those most important to the projectile's behavior.

The forces of gravity and inertia are usually of major importance in any hydrodynamic phenomena involving the free surface of a liquid. Hence these forces should be given primary consideration when attempting to model the cavity phase of an aircraft torpedo's flight. Two geometrically similar systems will be dynamically similar with respect to the gravitational and inertial forces if the ratio of these forces is the same in both systems. This ratio is known as the Froude number

$$Fr = \frac{v^2}{\ell g}$$

where: v = velocity of projectile
ℓ = a characteristic length
g = the acceleration of gravity

The size and shape of the cavity are determined by the physical and dynamic characteristics of the projectile, the orientation of the projectile in the cavity, and the cavitation number

$$k = \frac{p_o - p_c}{1/2\,\rho v^2}$$

where: p_o = absolute static pressure in the undisturbed liquid
p_c = absolute pressure within the cavity
v = velocity of the projectile
ρ = density of water

Therefore, the cavitation number should be the same for model and prototype systems in order to produce similar cavities. The condition that the Froude numbers in the two systems be identical requires that $(v_m/v_p)^2 = \lambda$, the ratio of linear dimensions of the model to the prototype. Substitution of this in the expression for the cavitation number shows that the ratio $(p_o - p_c)_m/(p_o - p_c)_p = \lambda$. Since the hydrostatic pressure is scaled in this ratio by the original requirement of geometrically similar trajectories, it follows that the gas phase pressure must also be scaled according to this linear scale ratio λ.

If air is used in the model work, changing the atmospheric pressure naturally changes the density of the gas. Valid Froude modeling requires that the atmospheric density be equal in both systems.[1] Experimental investigations of the entry behavior of vertically launched projectiles indicate that the time until surface closure of the cavity increases as the atmospheric density diminishes.[10] If closure is early, its time and location are important to the subsequent behavior of the projectile. If surface closure is late, it does not significantly affect the projectile behavior.[1,10] Photographic evidence from the launching tank has indicated that surface closure is sufficiently late to be neglected for the nose shapes, velocities, and entry angles thus far investigated. However, when surface closure is late, the cavity may neck down at some distance behind the projectile and throttle the flow of gas into the bubble. The pressure drop due to throttling is not modeled unless the atmospheric densities are equal in both systems.[1] However, in studies using small scale models with reduced atmospheric pressure, the total atmospheric pressure is small and any difference between that and cavity pressure due to the throttling would be of second order. Therefore, this effect of atmospheric density also has been neglected in the Controlled Atmosphere Launching Tank investigations.

After the cavity has been shed, the viscous effects upon the projectile become important. In order to maintain similarity between these effects, the ratio of the inertial to the viscous forces must be the same for both model and prototype. This ratio, known as Reynolds number, is

$$Re = \frac{v\ell\rho}{\mu}$$

where μ = absolute viscosity of the liquid.

If the same liquid is used for both model and

prototype work, the velocity must be scaled as λ^{-1} in order to satisfy the Reynolds criterion. Obviously, Reynolds and Froude scaling cannot be satisfied simultaneously if water is used in the model work. Wind and water tunnel tests indicate that the lift and moment acting on submerged bodies are very nearly independent of viscous effects if the Reynolds number (based upon length) is well above $10.^{6}$ Skin friction, however, is a function of Reynolds number and would cause greater deceleration in the Froude-scaled model than in the prototype. Therefore, similarity cannot be expected between the Froude-scaled model and the prototype beyond the cavity stage.

The forces occurring when the torpedo initially strikes the water surface depend upon the elastic properties of the water, for the force upon the nose of the projectile is

$$F = \rho c V A$$

where

V = velocity normal to the water surface
c = velocity of sound in water = $(E/\rho)^{1/2}$
A = area of contact projected normal to V
E = bulk modulus of water

and any dependence of c upon V is neglected. The Mach criterion, which must be satisfied to maintain similarity of the elastic forces, represents the ratio of inertial to elastic forces

$$M = \frac{V}{c}$$

If the liquid is not changed, this modeling law requires equal velocities as opposed to the $\lambda^{1/2}$ scaling necessary in the Froude system. So long as water is used in the Froude-scaled model system, the impact forces on the model will be too small by a factor of $\lambda^{1/2}$. However, since the Mach number is low and the impact stage of water entry very brief, [12] the unscaled elasticity of the water does not significantly affect the trajectory. On the basis of similar reasoning, the elasticity of the model itself can be neglected as well.

The effects of surface tension are insignificant compared with the forces of inertia and gravity for all except extremely small-scaled, low-velocity work. Therefore, in this work of modeling, the cavity would be independent of surface tension. The surface closure of any such cavity, however, might be affected, since the inertia of the atmospheric gas and the surface tension are of the same order of magnitude.

BIBLIOGRAPHY

1. Levy, Joseph and Kaye, John, "Effect of Atmospheric Pressure on Entry Behavior of Models of the Mark 13-6 Torpedo with Standard Head (Head F) and One Finer Head (Head I)", Hydrodynamics Laboratory, California Institute of Technology, Report No. N-59, Jan. 1949.

2. Levy, Joseph and Kaye, John, "Preliminary Studies of Effect of Atmospheric Pressure on Trajectory of 2-inch Correlation Model of Mark 13-6 Torpedo", Hydrodynamics Laboratory, California Institute of Technology, Report No. M-59, March, 1948.

3. Mason, M. and Slichter, L.B., "Water Entry and Underwater Ballistics of Projectiles", OSRD Report No. 2551, 1946.

4. Lindvall, F.C. and others, "Aircraft Torpedo Development and Water Entry Ballistics", OSRD Report No. 2550, 1946.

5. Cornelison, E.D. and Waugh, J.G., "Velocity-Distance, Velocity-Time, and Distance-Time Curves for Underwater Travel of Various Torpedoes", Memo NOC 48.2, Sept. 1945.

6. Wayland, H., "Model Correlation", T.L.D. 343-1, T.L.P. 1, Memo.

7. Eisenberg, P., and Pond, H.L., "Water Tunnel Investigations of Steady State Cavities", DTMB Report No. 668.

8. Daily, J.W., "Hydrodynamic Forces Resulting from Cavitation on Underwater Bodies", OSRD Section No. 6.1-sr207-2242, Hydrodynamics Laboratory Report No. ND-31.2, July, 1945.

9. Knapp, R.T., Levy, J., O'Neill, J.P., and Brown, F.B., "The Hydrodynamics Laboratory of the California Institute of Technology", Trans. Am. Soc. Mech. Engrs, Vol 70, No. 5, pp.437-457, July, 1948.

10. Gilbarg, D. and Anderson, R.A., "Influence of Atmospheric Pressure on Water Entry Phenomena", NOLR 1055, Dec. 2, 1946.

11. Slichter, L.B., "Modeling of Water Entry of Bombs and Projectiles", OSRD, NDRC, California Institute of Technology, March 31, 1944.

12. "Mathematical Studies Relating to Military Physical Research", Summary Technical Report of the Applied Mathematics Panel, NDRC, Vol. 1.

13. Birkhoff, Garrett, "Modeling of Entry into Water", NDRC, AMP Memo No. 42.9M, AMG-H No. 13, May, 1945.

14. "Torpedo Studies", Summary Technical Report of Div. 6, NDRC, Vol. 21.

15. Wayland, Harold, "Scale Factors in Water Entry", NAVORD 978, NOTS 105, April, 1947.

16. Knapp, R.T., "Nose Cavitation Ogives and Sphereogives", OSRD Section No. 6.1-sr207-1906, Hydraulic Machinery Laboratory Report No. ND 31.1, Jan. 1945.

17. Knapp, R.T., "Entrance and Cavitation Bubbles", OSRD Section No. 6.1-sr207-1900, Hydraulic Machinery Laboratory Report No. ND 31, Dec. 1944.